Progress in Oceanography 232 (2025) 103411

Contents lists available at ScienceDirect

Progress in Oceanography

journal homepage: www.elsevier.com/locate/pocean

A first look at xenophyophores (Rhizaria, Foraminifera) in the lower bathyal Bering Sea and abyssal areas adjacent to the Aleutian Trench

Andrew J. Gooday [a,b,*], Maria Holzmann [c], Jan Pawlowski [c,d]

[a] National Oceanography Centre, European Way, Southampton SO14 3ZH, UK
[b] Life Sciences Department, Natural History Museum, Cromwell Road, London SW7 5BD, UK
[c] Department of Genetics and Evolution, University of Geneva, Quai Ernest Ansermet 30, 1211 Geneva 4, Geneva, Switzerland
[d] Institute of Oceanology, Polish Academy of Sciences, Sopot 81-712, Poland

ARTICLE INFO

Keywords:
Protista
Deep-sea benthos
North Pacific
Seafloor images

ABSTRACT

Xenophyophores are an abundant component of the megafauna in parts of the equatorial and temperate North Pacific, but few records exist of these giant agglutinated foraminifera in northern North Pacific and adjacent waters. Here, we present a preliminary survey of xenophyophores from the bathyal Bering Sea (~3500 m depth) and at abyssal depths (4294–6555 m) adjacent to the Aleutian Trench, based on collected material, mainly fragments, and seafloor images. The dominant xenophyophore in the Bering Sea is a reticulated form that yielded DNA sequences identical to those obtained from *Syringammina limosa*, a species described from > 2700 km to the west in the Sea of Okhotsk. Also visible in seafloor photographs were various plate-like forms, often with upturned, undulating rims, but also branching plates and other more complicated morphotypes that probably represent distinct species. At stations close to the Aleutian Trench, core and epibenthic sledge samples yielded xenophyophores at seven of the 16 sampling sites. At least eleven morphospecies were recognised among those collected, none of which resembled *S. limosa* or the plate-like Bering Sea forms. Seafloor images revealed 16 fairly distinct domed or plate-like morphotypes three of these are possibly represented among the collected specimens, making a total of around 24 morphotypes or morphospecies. A few images show morphotypes similar to those seen in the Bering Sea. Our results suggests that xenophyophores are as diverse in the northern North Pacific as they are elsewhere in the Pacific Ocean.

1. Introduction

Our knowledge of xenophyophores in the North Pacific has grown considerably over the past 40 or so years and particularly during the last two decades. A series of studies described new species and genera from abyssal sites (>4000 m depth) at tropical latitudes in the Clarion-Clipperton Zone (CCZ) (Kamenskaya, 2005; Kamenskaya et al., 2015, 2017; Gooday et al., 2017a, b,c; Gooday et al., 2018; 2020b). These large agglutinated monothalamid foraminifera have also featured prominently in photographic surveys of megafauna across the CCZ (Kamenskaya et al., 2013; Amon et al., 2016; Simon-Lledó et al., 2019a; Simon-Lledó et al., 2019b). Earlier studies recorded undescribed xenophyophores at shallower depths on seamounts in the tropical western Pacific (07° to 19° N; Kaufmann et al., 1989) and eastern Pacific (10° to 31° N; Levin and Thomas, 1988). Xenophyophores have also been collected at abyssal and hadal sites at subtropical and temperate latitudes (28° to 38° N) in the vicinity of the Japanese Islands (Tendal et al., 1982; Swinbanks, 1982; Swinbanks and Shirayama, 1986; Lecroq et al., 2009; Hori et al., 2013; Tsuchiya and Nomaki, 2021). Further to the north, Voltski et al. (2018) described a new species, *Syringammina limosa,* from ~ 40° N in the Sea of Okhotsk (3500 m depth). The intriguing contribution of Levin et al. (2001) lists fragments of three xenophyophore species (*Psammina* sp., ?*Psammina* sp., and ?*Galatheammina* sp.) that were among > 1000 foraminiferal tests and test fragments that adorned the surface of an echinoid (*Cystochinus loveni*) recovered in a pushcore in the northern Gulf of Alaska (58° 51.7′N, 146° 2.9′W). This is probably the most northerly of any xenophyophore record.

Tendal (1972) listed seven abyssal stations beyond 40° N in the northern Pacific sampled during Russian *Vityaz* expeditions in the 1950s and 1960s that yielded xenophyophores. Five were off the Kamchatka Peninsula, but the two most northerly (*Vityaz* Stations 3357, 6088;

* Corresponding author.
E-mail address: ang@noc.ac.uk (A.J. Gooday).

https://doi.org/10.1016/j.pocean.2024.103411

Available online 12 December 2024

Table 1
Station details. Sampling devices are: BC = box corer; EBS = epibenthic sledge; MuC = multiple corer.

Station and deployment	Sampling device	Latitude (°N)	Longitude (°W)	Depth (m)
1–4	EBS	54° 31.513′-54° 31.231′	172° 36.226′-172° 38.041′	3517–3523
1–6	BC	54° 33.214′	172° 34.961′	3511
1–7	MuC	54° 33.213′	172° 34.949′	3511
1–10	EBS	54° 32.142′-54° 32.527′	172° 36.594′-172° 31527′	3499–3502
2–8	MuC	54° 32.213′	174° 37.642′	3652
4–8	MuC	51° 40.332′	170° 28.703′	4640
6–5	BC	50° 37.993′	169° 48.070′	5317
6–6	MuC	50° 37.932′	169° 48.078′	5316
7–6	MuC	51° 21.994′	168° 56.571′	6555
7–9	BC	51° 21.986′	168° 56.583′	6554
8–7	MuC	52° 21.971′	167° 05.283′	4612
9–14	MuC	51° 54.490′	166° 51.837′	6500
10–6	BC	51° 40.563′	166° 33.012′	5098
12–5	EBS	53° 35.535 – 53° 36.098′	162° 10.069′-162° 10.748′	4291–4305
12–7	MuC	53° 36.028	162° 10.659′	4305
12–8	MuC	53° 36.029	162° 10.666′	4304
12–9	EBS	53° 35.995 – 53° 36.750	162° 10.411′-162° 11.322′	4303–4320

51.5°N and ~ 54.0°N, respectively) were situated close to the Aleutian Trench, one near the eastern end and the other near the western end. Only species of *Stannophyllum* were recorded at these sites. A xenophyophore from two hadal stations in the Kurile-Kamchatka Trench was described by Saidova (1970, 1975) as *Astrorhizinella planata,* but later recognised as a xenophyophore and reassigned to the genus *Psammina* (Tendal, 1996; Kamenskaya and Saidova, 1998). In the Bering Sea to the north of the Aleutian Islands there are no confirmed xenophyophore records. Sagalevich et al. (1992) mention possible xenophyophores associated with bacterial mats at < 400 m depth on the north summit of the Piyp Submarine volcano (55.42°N 167.33°E), but their description – 'Very fine filaments up to 50 mm long, perhaps xenophiophores (sic.)' – is not convincing.

During the AleutBio cruise aboard the R/V *Sonne* in the summer of 2022 sampling was undertaken in the Bering Sea to the north of the Aleutian Islands and to the south in the region of the Aleutian Trench, within the framework of the AleutBio project (Brandt, 2022). Seafloor images were also obtained during the expedition using the ultra-high-definition towed Ocean Floor Observation System (OFOS) (Purser et al., 2019). These revealed that a reticulated xenophyophore was one of two dominant megafaunal organisms at three sites in the Bering Sea (Sigwart et al., 2023). The aim of the present paper is to build on this work by describing: 1) the morphology of four specimens of the Bering Sea xenophyophore together with molecular data identifying it as *Syringammina limosa* Voltski, Weiner, Tsuchiya & Kitazato 2018. 2) a small collection of mainly fragmentary material collected by benthic samplers, mainly in deeper water to the south of the Aleutian Islands, and 3) the xenophyophores seen in the OFOS images from both areas. Our observations provide new information about the abundance and diversity of xenophyophores in regions where these giant foraminifera are either poorly known or unreported, and also adds to our knowledge of their distribution in the wider Pacific Ocean.

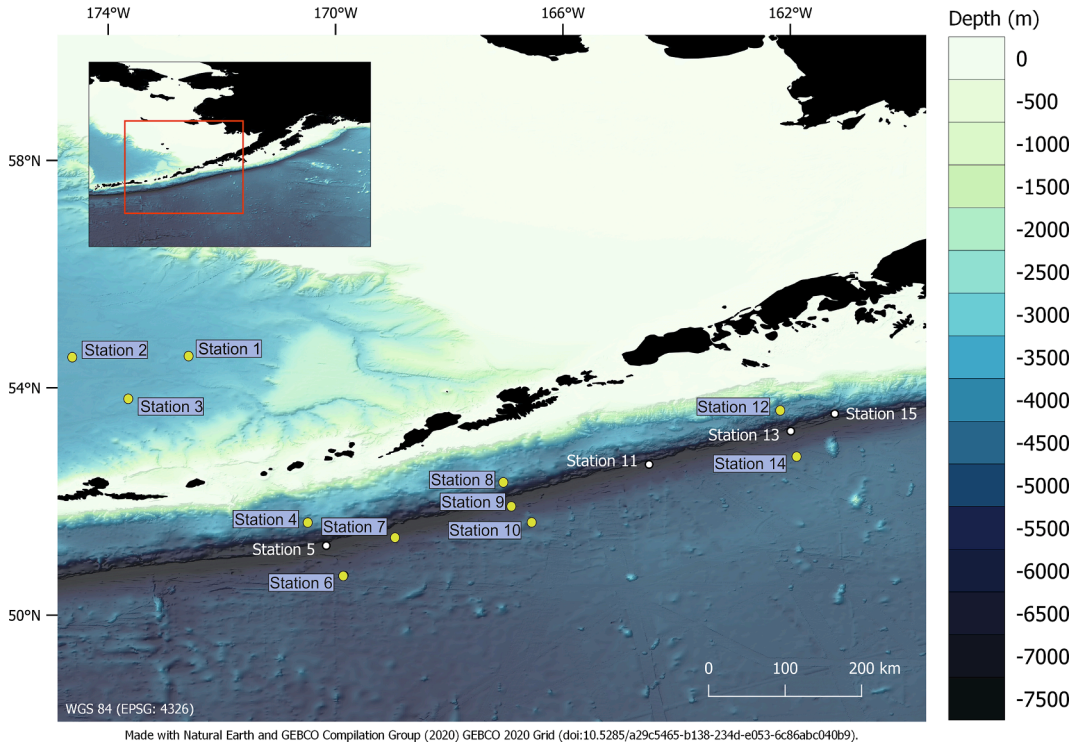

Fig. 1. Map of stations occupied during Sonne Cruise 293. Those where samples yielded xenophyophores and/or where xenophyphores were seen in OFOS images are highlighted. Based on a map created by Anne-Cathrin Wölfl and Kevin Kess.

Table 2
Overall xenophyophore densities and morphotype numbers in OFOS images. Data for number of frames, usable area, specimen numbers, and density (columns 4–6) for Stns 1–3 is taken from Supplementary Table S1 in Sigwart (2023). The numbers in column 6 are total numbers of specimens in all images combined and range per image. The densities in column 7 were calculated by dividing the total numbers of specimens (column 6) by the total usable area of the frames (column 5),

Station	Dive	Depth (m)	No. of frames	Usable area (m^{-2})	Specimens	Density (m^{-2})	Morphs
1	1	3507–3512	50	81.5	1078 (6–38)	13.2	3–4
2	2	3650–3653	50	90.8	477 (1–23)	5.25	2
3	3	3587–3588	48	86.7	477 (1–39)	5.50	2
4	4	4593–4610	51	79.5	133 (0–8)	1.67	9
6	5	5295–5327	50	110.5	94 (0–6)	0.85	9
8	6	4608–4610	51	89.0	40 (0–3)	0.45	7
10	7	5084–5093	50	133.0	126 (0–7)	0.95	9
12	8	4294–4309	50	131.7	11 (0–2)	0.08	2
14	9	4869–4875	50	125.2	16 (0–4)	0.13	6

2. Materials and methods

2.1. Shipboard methods

The study was carried out during the AleutBio expedition aboard the German research vessel *Sonne* (cruise SO293; 24th July to 6th September 2022). The overall aim of AleutBio is to compare faunas in the bathyal Bering Sea with those living at abyssal and hadal depths to the south of the Aleutian Arc in order to explore connectivity between these two regions and with more distant faunas to the south and west in the Sea of Japan, the Sea of Okhotsk and the Kuril-Kamchatka region, which were sampled during earlier expeditions (Brandt, 2022).

Seafloor images showing xenophyophores were obtained using a towed camera system, the Ocean Floor Observation System (OFOS), which utilizes a Full-HD video camera and a 45-megapixel mirrorless Canon EOS R5 still camera with a resolution of 8192 x 5464 pixels. A scale for the still camera is provided by three laser points that form a triangle on the seafloor and are separated by distances of 40 cm. The length of the conducting cable prevented the deployment of OFOS at depths greater than ~ 5500 m.

Specimens originated from five samples collected at two sites in the Bering Sea and 12 samples collected at seven sites to the south of the Aleutian Arc in the region of the Aleutian trench (Table 1). Three sampling devices were used: box corer, multicorer, and epibenthic sledge (Brandt, 2022). The USNEL-type box corer (BC) was fitted with a box measuring 50 x 50 cm. The multicorer (MuC) was fitted with twenty plastic tubes, each with an inner diameter of 9.4 cm and recovering a core with a surface area of 69.4 cm^2. The epibenthic sled was equipped with an epinet and a supranet, the latter mounted above the former in a metal frame. Both nets have side netting with a 500-μm mesh and cod ends with a 300-μm mesh.

Undamaged xenophyophores were recovered mainly by the BC. These were photographed before being carefully removed from the sediment surface, placed in a container with chilled seawater on a bed of ice. In the laboratory, xenophyophore fragments, most of which appeared to be dead, were picked from EBS residues, as well as from the sieve residues of surficial sediments (0–1 cm layer), mainly from MuCs. Intact xenophyophores or fragments thereof were photographed using either a hand-held Lumix DMC-LX10 digital camera or a DFK 37AUX226 USB Industrial Camera attached to a Leica MZ7 stereomicroscope. Several additional images were taken with a IMAGINGSOURCE digital camera (DFK 33UX264) mounted on a Nikon SMZ1270 stereomicroscope. These were stacked using the Nikon Instruments software NIS-Elements from live-view images to improve the depth of field (C. Chen written communication). Cytoplasm was dissected from fragments of *Syringammina limosa* and stored in RNAlater® for genetic analysis. Otherwise, the xenophyophores and their fragments were preserved in 10 % buffered formalin.

The location of stations at which either samples or OFOS photographs, or both were obtained are shown in Fig. 1.

2.2. Land-based methods

Following the cruise, additional photographs of xenophyophore fragments were taken in Southampton using an Olympus SZX7 stereomicroscope and an Olympus BH2 compound microscope, both equipped with a Canon 60D SRL digital camera, and in Geneva using a Leica M205 C motorized stereomicroscope equipped with a Leica DFC 450C camera.

Seafloor OFOS images taken at lower bathyal depths in the Bering Sea were examined to study the morphological diversity of xenophyophores, complementing density data published by Sigwart et al. (2023). OFOS was also deployed at six abyssal sites (4294–5327 m) adjacent to the Aleutian Trench. Images from these sites were analysed in order to determine the density and morphological diversity of xenophyophores on the seafloor in comparison with those from the Bering Sea. Density values were based on randomly selected images (usually 50) at each site. The method described by Sigwart et al. (2023) was followed as far as possible. Briefly, the area covered by each of the selected frames (which will depend on the distance of the camera above the seafloor) was calculated based on the average distance between the three laser points, spaced 40 cm apart. The frames were examined carefully in a systematic way. The number of xenophyophores in the inner, in-focus part were counted and densities calculated assuming that this in-focus area was 60.5 % of the total frame area (the proportion calculated by Sigwart et al., 2023). In Table 2 we report the number of frames analysed, their total usuable (in-focus) area (i.e., all frames combined), the total number of xenophyophores recognised, the range of numbers visible in individual images, and densities. Because single frames covered too small of an area to be considered as replicates, the mean densities at each site were then calculated by dividing the total number of xenophyophores in the 50 frames by the total in-focus area examined.

Every xenophyophore visible in the 50 carefully analysed frames was copied and the images assembled on Powerpoint slides. To obtain a more complete coverage of the morphotypes present at each site, several hundred additional frames were also viewed. All obvious xenophyophores seen were copied and added to the Powerpoint slides and the images assembled from each site were arranged, as far as possible, into different morphotypes. Because these additional frames were not analysed systematically to the same degree as the 50 that were randomly selected, the resulting data are regarded as semiquantitative.

2.3. DNA extraction, PCR amplification and sequencing

For the present study, four DNA extractions were obtained from *Syringammina limosa* using the DNeasy Plant Mini Kit (Qiagen). Each DNA extraction was marked by a unique isolate number. Successful semi-nested PCR amplification was carried out for a part of the 18S rRNA barcoding fragment of foraminifera (Pawlowski and Holzmann, 2014) using forward primers s14F3 (3′acgcamgtgtgaaacttg5′)-s17r (3′cggtcacgttcgttgc5′) for the first and primers s14F1

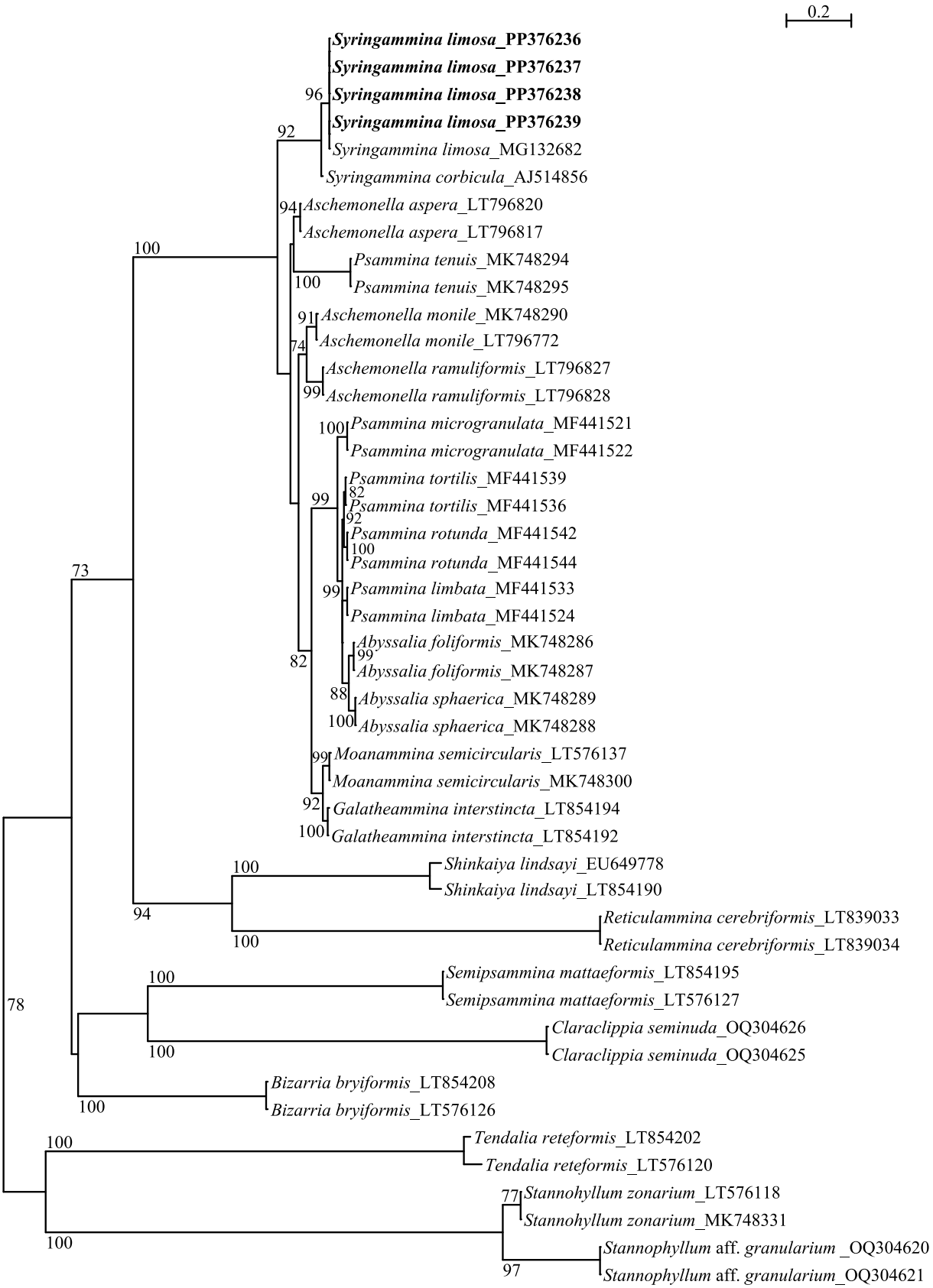

Fig. 2. PhyML phylogenetic tree based on the 3′end fragment of the SSU rRNA gene showing the evolutionary relationships of 44 monothalamid sequences. Specimens marked in bold indicate those for which sequences were acquired during the present study. The tree is unrooted. Specimens are identified by their accession numbers. Numbers at nodes indicate bootstrap values (BVs). Only BVs > 70 % are shown.

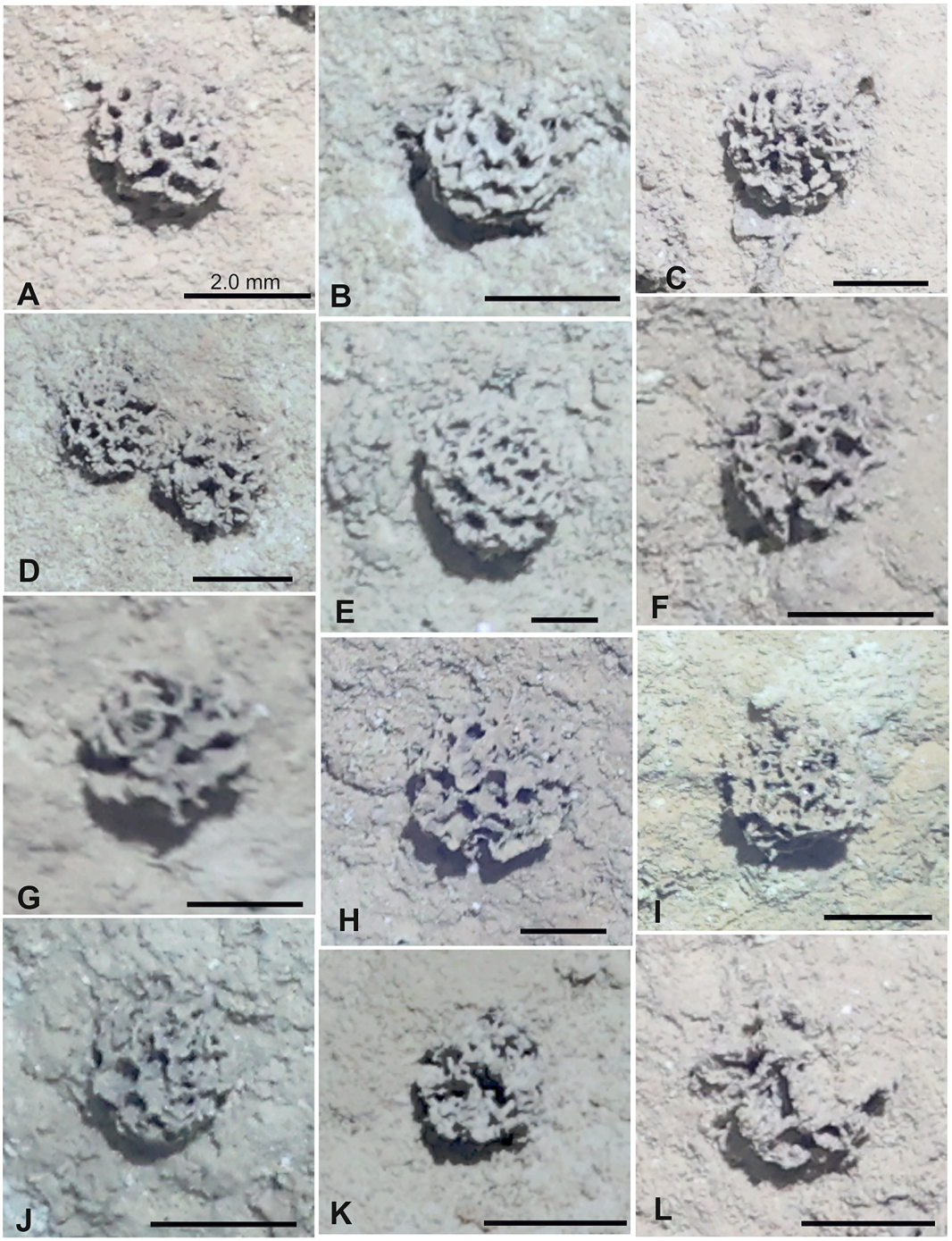

Fig. 3. *Syringammina limosa.* Specimens photographed on the seafloor at Stn 1 using the OFOS towed camera system. All scale bars = 2 cm.

(3′aagggcaccacaagaacgc5′)-s17r for the second amplification. Thirty-five and 25 cycles were performed for the first and the second PCR, with an annealing temperature of 50° C and 52° C, respectively (Holzmann, 2024). The amplified PCR products were purified using the Roti ®Prep PCR Purification Kit (Roth). Sequencing reactions were performed using the BigDye Terminator v3.1 Cycle Sequencing Kit (Applied Biosystems) and analyzed on a 3130XL Genetic Analyzer (Applied Biosystems). The resulting sequences were deposited in the NCBI/GenBank database. Isolate and Accession numbers are specified in Supplementary Table S1.

2.4. Phylogenetic analysis

The obtained sequences were added to 42 xenophyophore sequences (Supplementary Table S1) that are part of the publicly available 18S database (NCBI/Nucleotide; https://www.ncbi.nlm.nih.gov/nucleotide/). All sequences were aligned using the default parameters of the Muscle automatic alignment option as implemented in SeaView vs. 4.3.3. (Gouy, et al. 2010). The alignment contains 46 untrimmed sequences with 1113 sites used for analysis. The phylogenetic tree (Fig. 2) was constructed using maximum likelihood phylogeny (PhyML 3.0) as implemented in ATGC: PhyML (Guindon et al. 2010). An automatic model selection by SMS (Lefort et al. 2017) based on Akaike Information Criterion (AIC) was used, resulting in a GTR + G substitution model being selected for the analysis. The initial tree is based on BioNJ. Bootstrap values (BV) are based on 100 replicates.

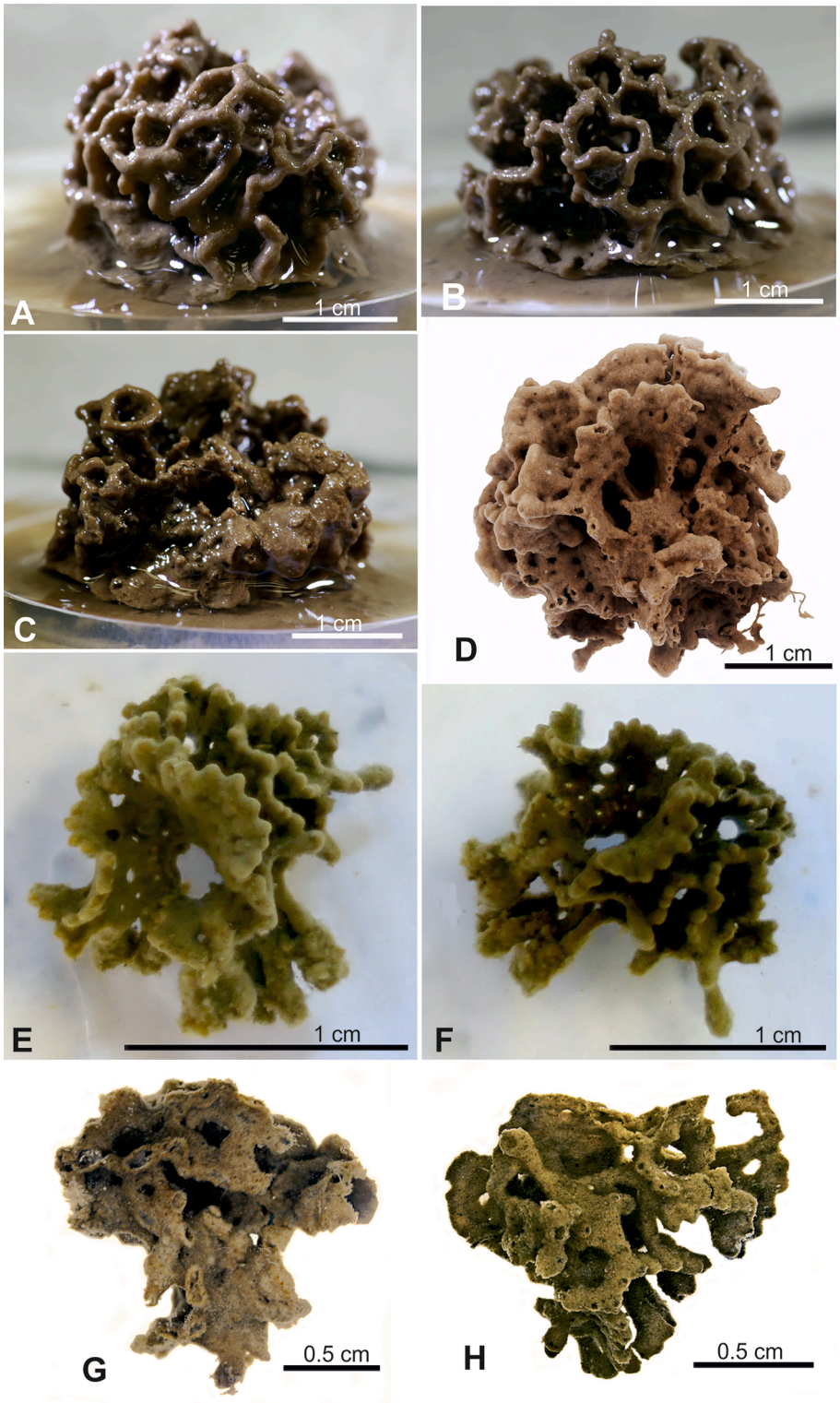

Fig. 4. *Syringammina limosa,* shipboard photographs. (A¬D) Sequenced specimen from Stn 1 box core. Collection Foraminifera marin resent-SMF 1. (A¬C) Side views. (D) Top view. (E, F) Specimen from Stn 2. Collection Foraminifera marin resent-SMF 2. (G) Small specimen from Stn 1. Collection Foraminifera marin resent-SMF 3. (H) Small specimen from Stn 1. Collection Foraminifera marin resent-SMF 4. (D, G, H) Focus merged images courtesy of Chong Chen.

3. Results

3.1. Bering Sea xenophyophores: Syringammina limosa

As reported previously by Sigwart et al. (2023), the most abundant megafaunal organism visible in OPHOS photographs from Stn 1 in the Bering Sea was the xenophyophore *Syringammina limosa.*

3.1.1. Seafloor images of S. limosa

This species is abundant in OFOS images from Stns 1–3. Fifteen images from Stn 1 were examined in detail and all 173 specimens that we felt confident belonged to this species were measured. The length

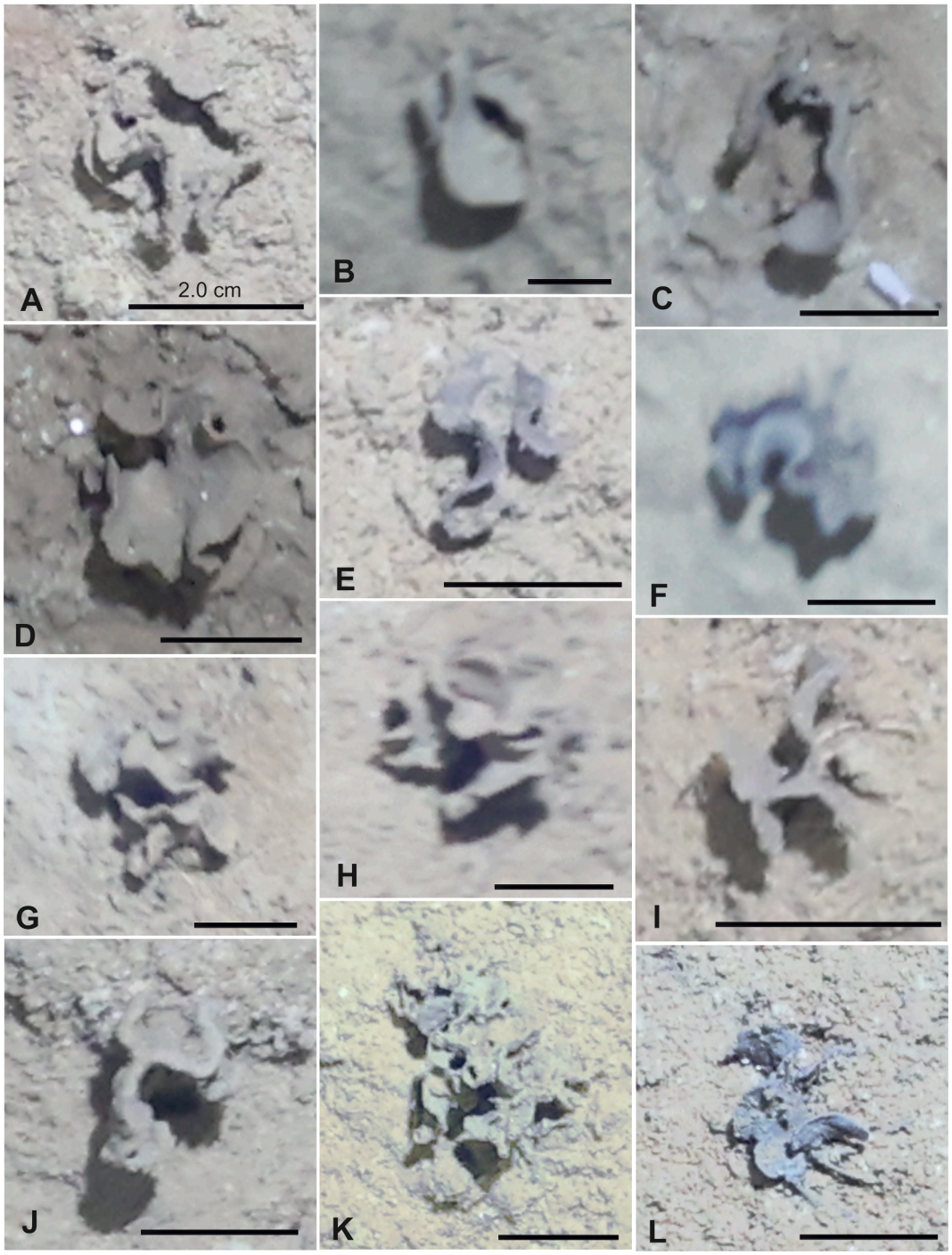

Fig. 5. Plate-like xenophyophore morphotypes in OFOS seafloor images from the Bering Sea (Stn 1). (A¬F) Relatively simple forms. (G, H) more complex forms. (I, J) Simple branched plates. (K, L) Complicated forms with irregular plate-like elements. All scale bars = 2 cm.

(maximum dimension) ranged from 0.67 to 4.7 cm with 59 % of specimens measuring 2–3 cm; the width (minimum dimension) ranged from 0.54 to 4.5 cm with almost 58 % measuring 1.5–2.5 cm; the L/W ratio ranged from 1 to 1.84 with 57 % between 1 and 1.2.

The images showed specimens apparently distributed randomly across the seafloor, although closely-spaced pairs were occasionally observed (Fig. 3D). They display a substantial degree of morphological variation. Some have a fairly regular reticulated structure, although the reticulations are smaller in some cases than in others (Fig. 3A-G) and smaller and larger reticulations are sometimes combined within a single test (Fig. 3E, F). Others display a tendency for the reticulated structure to become less well organised (Fig. 3I, J), sometimes with very small reticulations (Fig. 3I) and finally breaking down into narrow, irregular ridges that lack any clear organisation, giving the test a chaotic appearance (Fig. 3K, L). See Supplementary Fig. S1 for further examples of specimens with disorganised tests.

According to Sigwart et al. (2023), densities of *S. limosa* in these images range from around 5 to 26.1 individuals.m^{-2} (median value ~ 13 individuals.m^{-2}) at Stn 1 but are much lower (~1–14 ndividuals.m^{-2}) at Stns 2 and 3.

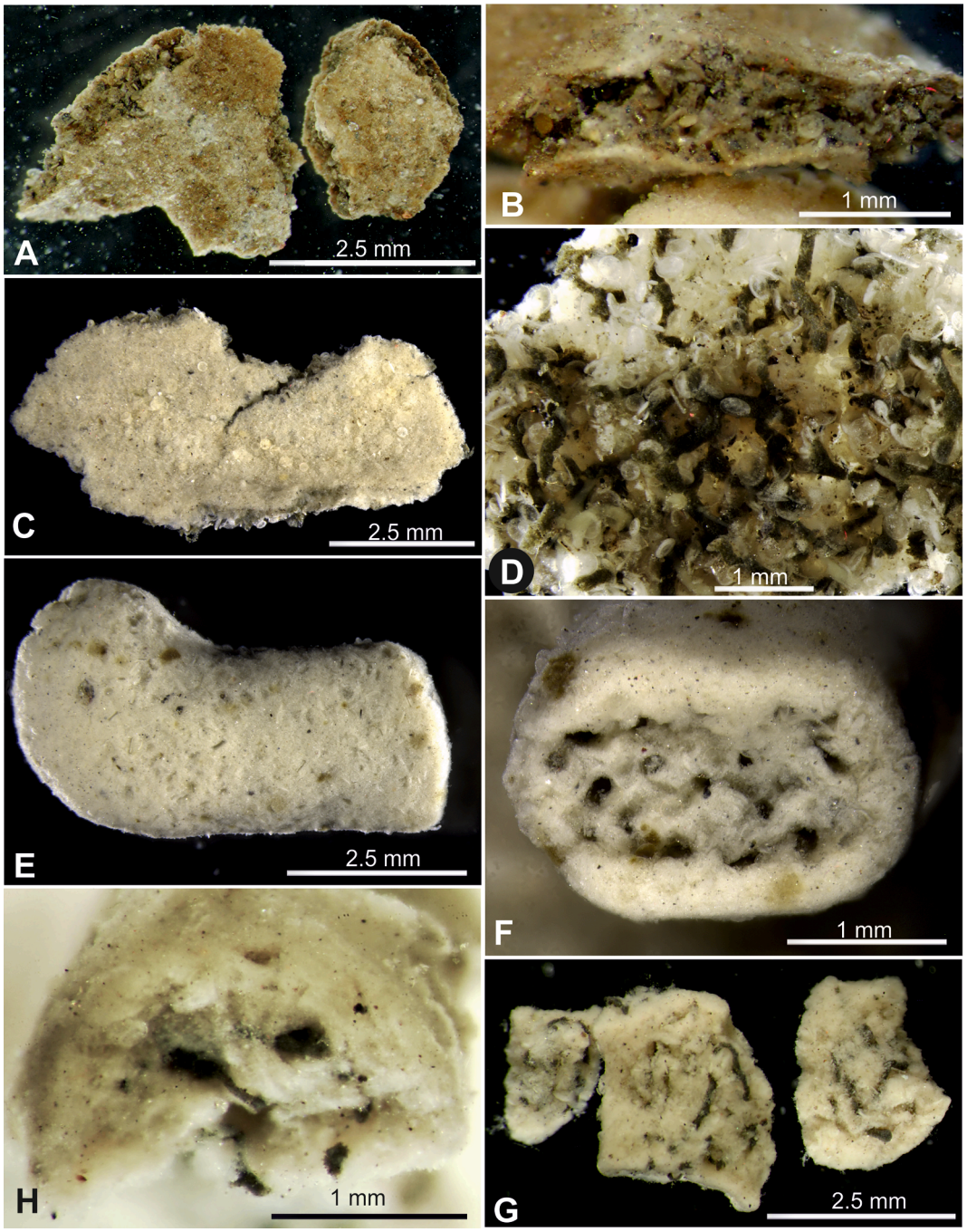

Fig. 6. Xenophyophores from Bering Sea (Stn 1). (A) Form 1, two plate-like fragments from Stn 1–2, MuC#2. (B) Form 1, broken edge of larger fragment. (C, D) Form 2, plate-like fragment with agglutinated diatoms from Stn 1–4, EBS#1. (C) Fine-grained outer surface with scattered diatoms. (D) Detail of inner surface with numerous diatoms and stercomare. (E, F) Form 3, subcylindrical fragment with internal stercomare-filled channels from Stn 1–4. (E) Outer surface with projecting diatoms (seen edge-on). (F) Broken end showing internal channels. (G, H) Fragments from Stn 1–10, EBS#2. (G) Side views showing internal channels filled with stercomare. (H) End view of fragment showing internal channels in cross section.

3.1.2. Collected specimens of S. limosa

Four specimens were obtained in two box-core samples: specimen 1, 3 and 4 from Stn 1 and specimen 2 from Stn 2. All are deposited in the Naturmuseum Senckenberg, Frankfurt, under the following reference numbers: Collection Foraminifera marin rezent – SMF 1¬4.

(i) Specimen 1: Collection Foraminifera marin rezent – SMF 1 (Fig. 4A-D).

The test sat directly on the sediment surface. It is roughly hemispherical, 3.4 cm long, 2.8 cm wide and 2.3 cm high, and lacks any obvious root-like structures. It has a complex structure comprised largely of perforated plates, apparently formed by the merging of tubular elements. This is seen most clearly in the view from above, which shows a somewhat asymmetrical test (Fig. 4D). On one side, the perforated plates are arranged in several variably developed, concentric arcs around a relatively large open space. The perforations of the plates tend to be arranged in zones parallel to the margin, creating a pattern of radial bars separated by open spaces. When viewed laterally from this side (Fig. 4A, B), the outer edges of the plates form circuits, creating a reticulated structure with roughly polygonal openings of different sizes. The edges themselves are curved, undulating or lobate, and often

somewhat thickened. On the other side, the test structure is rather disorganised, both in side view (Fig. 4C) and top view (Fig. 4D). The test wall is soft, fine-grained with scattered larger grains including biogenic and darker mineral particles.

The test interior appears devoid of internal particles. It is partly occupied the stercomare, which forms elongate masses running along the branches of the test. The granellare is whitish, branched and usually between 50 and 100 μm wide.

(ii) Specimen 2: Collection Foraminifera marin rezent – SMF 2 (Fig. 4E, F).

The test is ~ 2.5 cm diameter and 1.5 cm high. It is dominated by curved plates perforated by open spaces of varying sizes and shapes that merge into reticulated bars where the open spaces dominate. The plates often have wavy lobate outer margins. When viewed from above (Fig. 4E) the test appears asymmetrical. On one side, a relatively large, perforated plate forms an incomplete circuit around a space that is open towards the periphery of the test. Below this several bar-like projections extend horizontally, before widening into club-like, sometimes flattened, structures with fluffy surfaces that contrast with the smooth surface of the rest of the test (Fig. 4F). These projections were located below the sediment surface when the specimen was still undisturbed in the core. On the opposite site of the test, the plates are closely spaced and tend to break up into reticulated bars. They form two or three complete circuits that define deep voids. The test is quite soft with a certain degree of flexibility.

(ii) Specimens 3 and 4: Collection Foraminifera marin rezent – SMF 3 and 4 (Fig. 4G, H). These small specimens were recovered relatively intact, although their original orientation is not clear. As seen on the ship after removal from the core, specimen 3 measured ~ 1.60 x 1.70 cm and comprised a rather densely reticulated combination of plate- and bar-like elements. Specimen 4 measured ~ 1.40 x 0.75 cm and more distinct bar-like elements, some of them reticulated.

3.1.3. Remarks

The two larger specimens (1 and 2) have rather different morphologies. Both comprise an asymmetrical system of perforated plates that merge into reticulated bars, but specimens 1 is larger and more complicated than specimen 2 with a more obvious reticulated structure, at least when viewed from the side. Specimen 2, on the other hand, has plates with more strongly lobate margins. The morphology of specimen 1, in particular, is consistent with the detailed description given by Voltski et al. (2018). In both cases, there is a tendency towards asymmetry of the test structure, as also shown in some of our OFOS images (Fig. 3; Supplementary Fig. S1). The chaotic pattern of test elements described by Voltski et al. (2018, Plate 2A, B therein) in one specimen is mirrored by some of those seen in OFOS images (Fig. 3K, L).

3.1.4. Molecular characterisation

Sequences derived from specimen 1 differed in only one nucleotid position from the sequence of *Syringammina limosa* described from the Sea of Okhotsk (Fig. 2). This species (96 % BV) branches with *S. corbicula*, and the group is strongly supported (92 % BV). Sequence length of *S. limosa* amounts to 428 nucleotides, the GC content is 33 %.

3.1.5. Molecular phylogeny

The xenophyophore sequences included in the phylogenetic tree (Fig. 2) cluster in four clades with *Stannophyllum* spp. and *Tendalia reteformis* branching at the base. The monophyly of four clades is sustained by bootstrap values, except for clade 3 containing *Semipsammina mattaeformis*, *Claraclippia seminuda* and *Bizarria bryiformis*. Species represented by two or more sequences are supported by high bootstrap values (82–100 %).

The first clade contains fourteen taxa. Within this clade, the branching of *Syringammina limosa* and *S. corbicula* is highly supported (92 % BV). The grouping of *Psammina microgranulata, P. tortilis, P. rotunda, P. limbata, Abyssalia foliformis, A. sphaerica, Moanammina. semicircularis* and *Galatheammina interstincta* is also well supported (82 % BV). *Aschemonella aspera* and *P. tenuis* branch as sister, but without a strong support. The second clade contains *Shinkaiya lindsayi* and *Reticulammina cerebriformis*, both strongly supported (94 % BV). *Stannophyllum zonarium*, *S.* aff. *granularium* and *T. reteformis* branch at the base of all other clades, their branching is moderately supported (78 %BV).

Table 3
Abundance of different xenophyophore morphotypes in OFOS images. The abundance categories are based on the 50 images analysed in detail and a larger number of additional images that were examined less systematically and only obvious xenophyophores noted. The categories therefore give only a general indication of the relative importance of different morphotypes. 1 = Singleton; U = 2–10; C = 11–50, VC = >50.

Station number	4	6	8	10	12	14	Figure
OFOS dive number	**4**	**5**	**6**	**7**	**8**	**9**	
Basically plate-like morphotypes: 420 specimens (44.7 %)							
Plate-like fairly complex, generally compact	0	VC	C	C	C	C	7
Plate-like thin, branching, irregular shape	C	1	0	U	0	0	8A¬C
Plate-like simple, erect, or flat with raised rim	C	C	C	C	U	C	8D¬J
Plate-like sinuous, pale extremities, compact	0	U	0	0	0	0	8 K¬M
Plate-like flat-lying, very irregular margin	U	0	0	0	0	U	S3A-C
Plate-like highly irregular, spiky margin	0	U	0	U	0	0	S3D-G
Plate-like flat-lying, highly lobate margin	1	0	0	0	0	0	S3H
Plate-like stalked	1	0	0	0	0	0	S3I
Total numbers seen in images	**101**	**118**	**66**	**75**	**19**	**41**	
Regular and irregular domes and lumpy morphotypes: 217 specimens (23.1 %)							
Dome Finely reticulated	0	C	0	VC	0	U	9A-C
Dome coarsely reticulated	0	0	U	0	0	0	S4A-C
Dome with finely reticulated lobed bars	0	U	0	2	0	0	S4D-E
Dome dark with paler-tipped outgrowths	0	1	0	0	0	0	S4F
Dome with sinuous plates, some reticulations	C*	0	C	0	0	0	9D-F
Regular-irregular domes, surface rough, uneven	C*	0	C	C	0	0	9G-L
Total numbers seen in images	**34**	**53**	**11**	**113**	**0**	**6**	
Pale smooth morphotype: 175 specimens (18.6 %)							
Simple or branching	VC	C	U	C	0	C	10A-F
Reticulated	C	0	U	U	0	U	10G-I
Total numbers seen in images	**84**	**11**	**15**	**39**	**0**	**26**	
Indeterminate	11	34	35	13	19	15	
Grand Total seen in images	**230**	**216**	**127**	**240**	**38**	**88**	

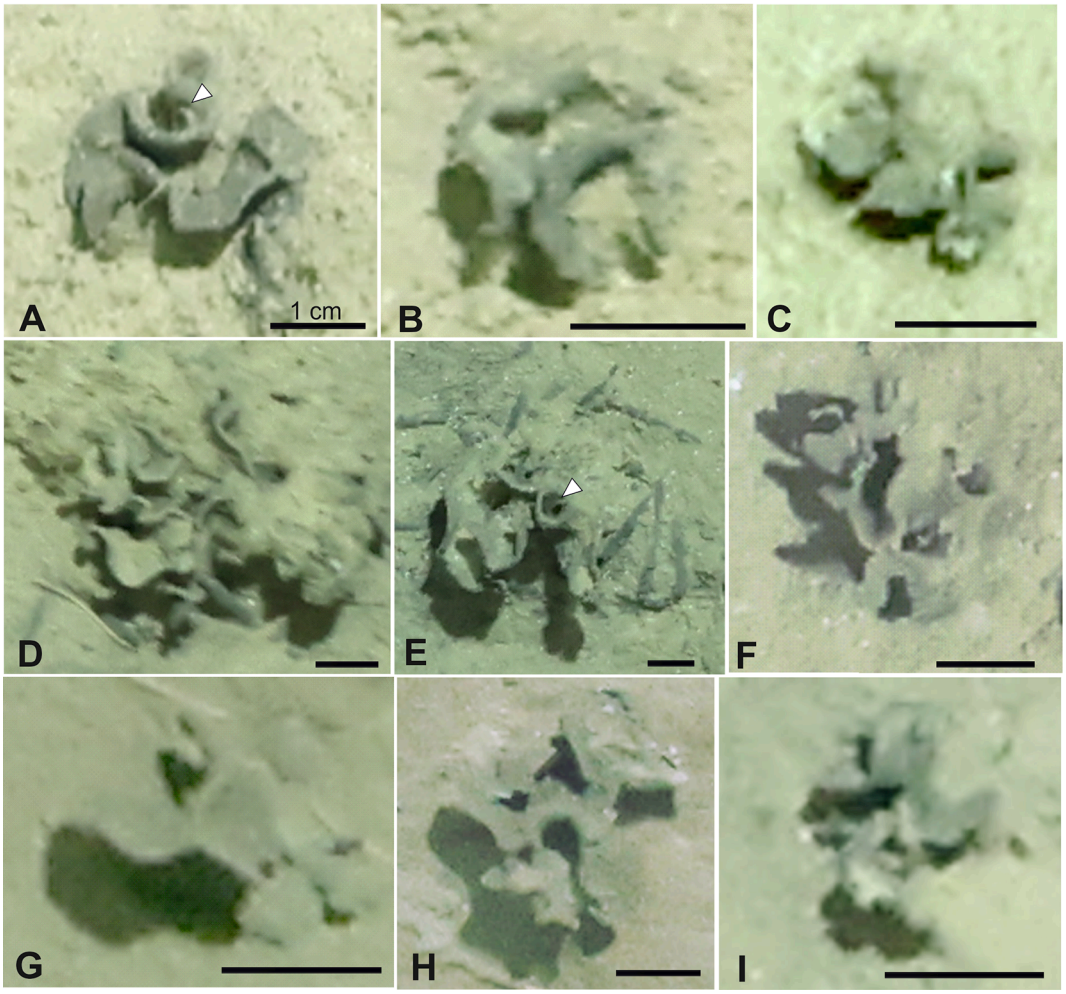

Fig. 7. Xenophyophores morphotypes with fairly complex, plate-like tests in OFOS seafloor images from sites to the south of the Aleutian Islands. (A¬C) Stn 6, Dive 5. (D¬E) Stn 10, Dive 7. (F¬H) Stn 8, Dive 6. (I) Stn 14, Dive 9. Arrowheads indicate chimney-like features. All scale bars = 1 cm.

3.2. Other Bering Sea xenophyophores

3.2.1. Appearance in seafloor images

In addition to *S. limosa,* a total of 36 plate-like xenophyophores are visible in the fifteen OFOS images from Stn 1 that were examined in detail. The specimens range from 1.1 to 4.0 cm (usually 2.0–2.5 cm) long, 0.9 to 3.6 cm (usually 1.0–2.5 cm) wide, with length/width ratios between 1.0 and 1.8 (usually 1–1.4). Several morphotypes can be tentatively distinguished, suggesting that a number of species are represented. Relatively simple, flat-lying, plate-like tests of varying shapes, but usually with the central part depressed and a raised, undulating rim, are most common (Fig. 5A¬F; Supplementary Fig. S2A¬F). The folds are sometimes quite tight, creating incomplete funnel-like structures, but the sides of such features do not merge to form complete circuits. Some other plate-like specimens are more complicated, comprising multiple branched plates (Fig. 5G, H; Supplementary Fig. S2G¬I)). Two other plate-like morphotypes are recognisable. Type 1 (Fig. 5I, J; Supplementary Fig. 2J¬L) have a relatively simple vertically orientated plate that branches once or twice, the branches usually being somewhat curved. Those grouped as Type 2 (Fig. 5K, L) are much more complicated, comprising multiple curved or irregular plate-like elements. One specimen includes a tubular, funnel-like structure. The plates appear thinner than in other forms and their arrangement is quite chaotic without any obvious pattern.

3.2.2. Collected fragments

Only a few small xenophyophore fragments were obtained from the samples collected at Stn 1 (Fig. 6). Three forms could be recognised but the material was too fragmented for any attempt to be made to link them with those seen in the OFOS images. See Appendix A for more detailed descriptions of these forms.

Plate-like Form 1 (Fig. 6A, B): two small, basically plate-like fragments with thin, well-defined wall.

Plate-like Form 2 (Fig. 6C, D): pale, plate-like fragments having finely agglutinated wall with scattered diatoms and interior rich in diatoms.

Bar-shaped form (Fig. 6E, F): single elongate, flattened, bar-shaped fragment with a pale, fine-grained test and solid interior punctuated by stercomare-filled channels.

3.3. Xenophyophores from the Aleutian Trench region

3.3.1. Seafloor images

Xenophyophores were present in images from all six sites at which OFOS was deployed near the Aleutian Trench. Their overall density was highest (1.67 ind.m^{-2}) at Stn 4 and lowest at Stns 12, and 14 (0.08 and 0.13 ind.m^{-2}, respectively), with Stns 8, 6 and 10 yielding intermediate values (0.45, 0.85, 0.95 ind.m^{-2}, respectively) (Table 2). The numbers of specimens per frame ranged from 0 to 8. In total, 16 morphotypes were recognised, with between 2 (Stn 12) and 9 (Stns 4, 6, 10) being represented at particular sites. However, some displayed considerable

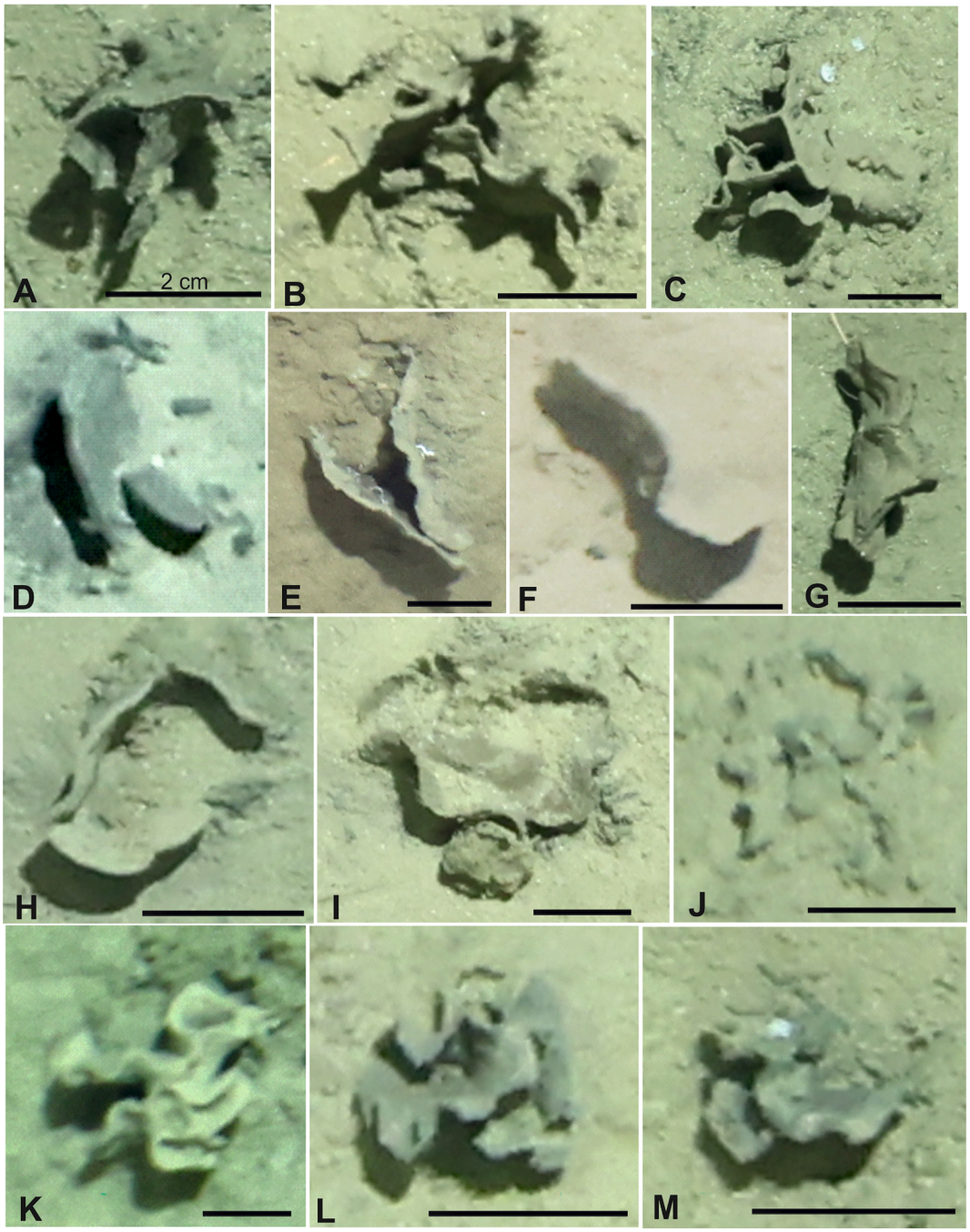

Fig. 8. Plate-like xenophyophores morphotypes in OFOS seafloor images from sites to the south of the Aleutian Islands. (A¬C) Very thin, branched plates, Stn 6, Dive 5. (D¬G) Simpler plates that project vertically. (D¬F) Stn 14, Dive 9. (G) Stn 4, Dive 4. (H¬J) Simpler plates that lie horizontally with raised rims. (H, I) Stn 10, Dive 7. (J) Stn 6, Dive 5. (K¬M) Compact form comprising sinuous plates with pale extremities, Stn 6, Dive 5. All scale bars = 2 cm.

variation and probably encompassed more than one species. The morphotypes could be assigned to the following three broad categories: predominantly plate-like tests, regularly domed and irregularly lumpy tests, and smooth pale tests constructed from relatively thick bar- or plate-like elements. These represented 44.7 %, 23.1 % and 18.6 %, respectively, of the specimens in the images, with the remaining 13.6 % being considered indeterminate (Table 3).

(i) Predominantly plate-like tests. Forms with fairly complex, compact tests comprising relatively thin plates were seen in OFOS images at all stations, except for Stn 4 (Fig. 7). The plates branch to varying extents and follow a curved or sinuous course with circular chimney-like features sometimes present (Fig. 7A, E). This morphotype displays considerable variability. Some specimens are more complex than others (e.g., Fig. 7D vs 7G), making it likely that the morphotype includes

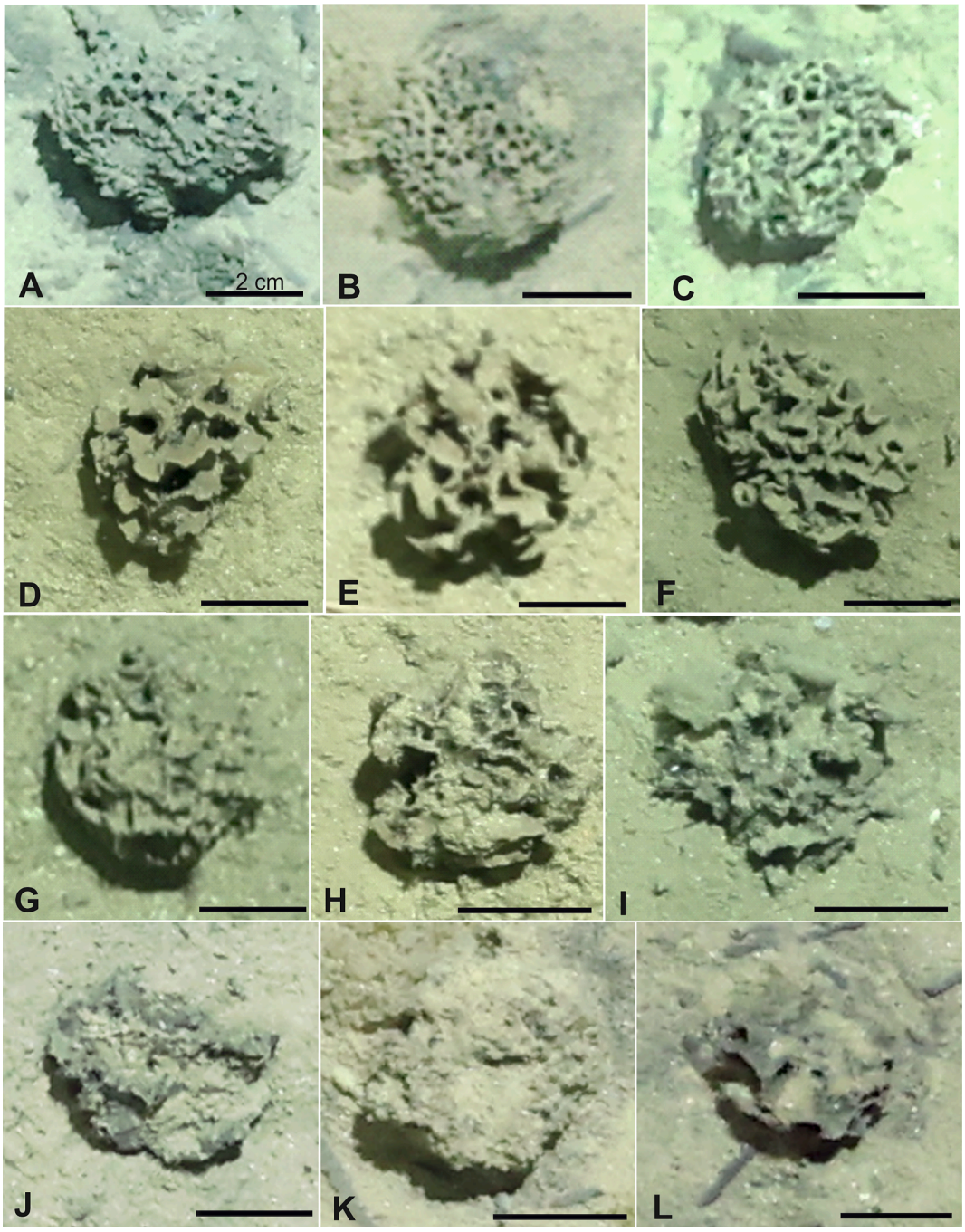

Fig. 9. Domed xenophyophores morphotypes in OFOS seafloor images from sites to the south of the Aleutian Islands. (A¬C) Finely reticulated domed tests. Stn 10, Dive 7. (D¬F) Regular domes with sinuous partly reticulated plates. Stn 4, Dive 4. (G¬I) Dome with highly irregular surface structure including jagged ridges. Stn 4, Dive 4. (J¬L) Irregular domes with very rough, uneven surface devoid of major features. Stn 10, Dive 7. A and B have sediment lodged within the structure and are probably dead. All scale bars = 2 cm.

several species, although it is not possible to distinguish morphologically consistent forms. A similar form has a very irregular growth pattern and comprises vertically orientated plates that are particularly thin and sometimes branch in a rather rectangular fashion (Fig. 8A-C). It is most common at Stn 4 (Dive 4) but also present at Stn 10 (Dive 7) with one example at Stn 6 (Dive 5). Simpler plate-like forms that either project from the sediment surface (Fig. 8D-G) or lie flat on it (Fig. 8H-J) are fairly common and represented at all stations. Some of the flat-lying plates have an upturned rim and resemble an irregular water lily leaf, while the plate shown in Fig. 8D is thicker than other projecting plates (Fig. 8E-G). These simpler plates therefore may also represent several species.

The other morphotypes that we include in the plate-like category are uncommon. A compact form that comprises several thicker, sinuous plates with pale rounded extremities is represented by three specimens at Stn 6 (Dive 5) (Fig. 8K-M). A few flat-lying specimens featuring very irregularly jagged margins were seen at Stn 4 (Dive 4), with other possible examples at Stn 14 (Dive 9) (Supplementary Fig. S3A-C). A distinctive morphotype in which the test gives rise to numerous elongate, spiky processes that project out in different directions was represented at Stns 6 and 10 (Dives 5 and 7) (Supplementary Fig. S3D-G). This interesting form is not really plate-like, except perhaps in the central

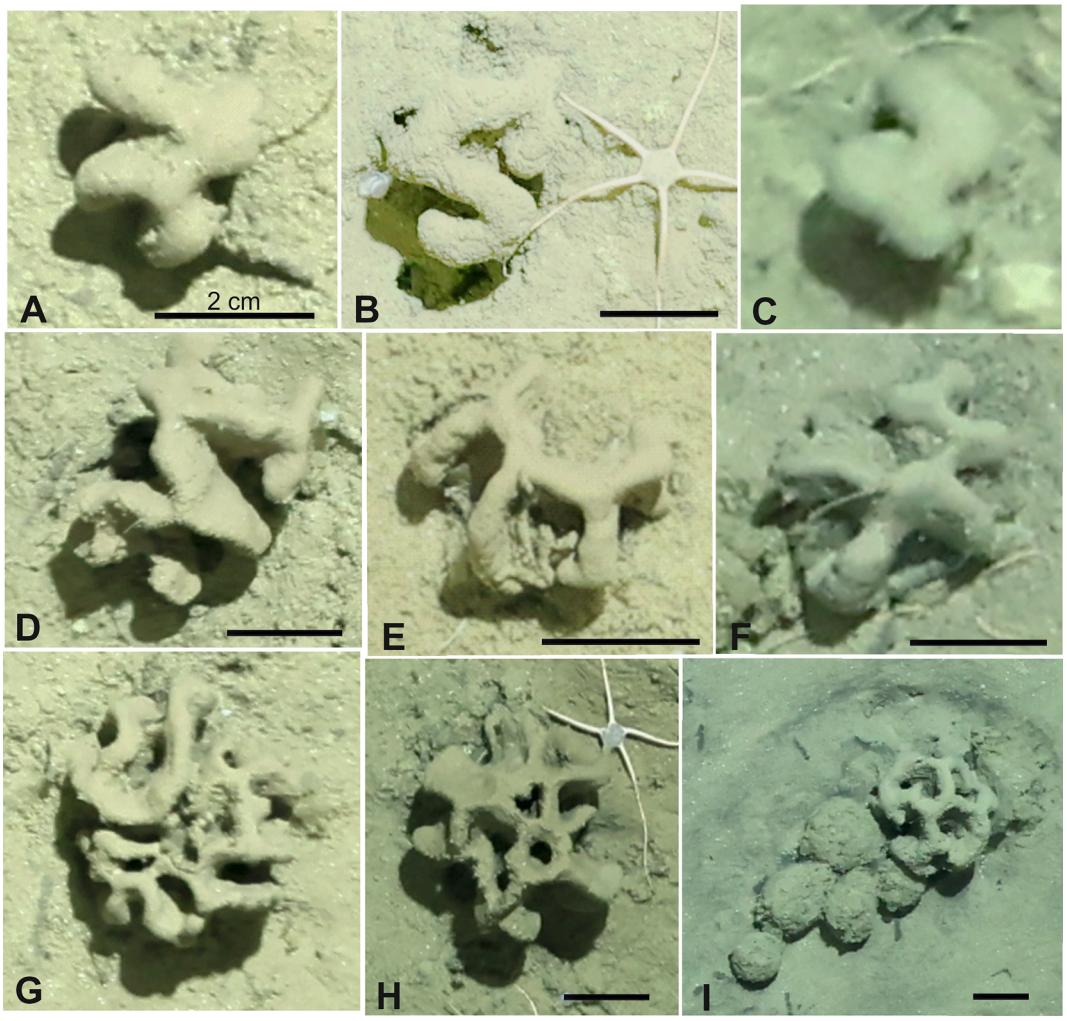

Fig. 10. Smooth, pale tests with wide bar or plate-like elements in OFOS seafloor images from sites to the south of the Aleutian Islands. (A¬C). Simple, unbranched specimens. (A, B) Stn 4, Dive 4. (C) Stn 10, Dive 7. (D¬F) Branched specimens. (D, E) Stn 4, Dive 4. (F) Stn 10, Dive 7. (G¬I) More complex domed specimens. (G, H) Stn 4, Dive 4. (I) Stn 14, Dive 9). All scale bars = 2 mm. Scales were not available for C and G.

part of the test, but was included in this category for convenience. A single specimen in an OFOS image from Stn 4 had an irregularly lobate margin (Supplementary Fig. S3H). Another singleton appears to be the only example of an upstanding stalked plate, although the photograph is rather indistinct and shows a very oblique view (Supplementary Fig. S3I).

(ii) Domed or lumpy morphotypes. These were represented at all stations except Stn 12 (Dive 8). There are three main morphotypes. The first, which was particularly common at Stn 10 (Dive 7), is characterised by a finely reticulated, more or less regularly domed test (Fig. 9 A-C). The second main morphotype is a regular dome comprising sinuous plates with some degree of reticulation (Fig. 9D-F). Typical specimens of this form occur at Stns 8 (Dive 6) and notably at Stn 4 (Dive 4). The third main morphotype is not well defined. Specimens seen in images from Stn 4 have a distinct but highly irregular surface structure that includes jagged ridges (Fig. 9G¬I). There are no clear reticulations, although one or two circular features, defined by ridges, are sometimes present. These resemble some irregular forms of *S. limosa* in Bering Sea images (Fig. 3K, L; Supplementary Fig. S1). Those at Stns 8 and 10 (Dives 6 and 7) are lumpy with a surface that is very rough and uneven but devoid of major features (Fig. 9J¬L). At least some of these could possibly be degraded specimens of the finely reticulate morphotype that is common at Stn 10 (Dive 7). Other dome-like forms are uncommon. OFOS images from Stns 4 and 8 (Dives 4 and 6) include a few rather coarsely reticulated specimens that appear distinct from other abyssal domed forms to the south of the Aleutian Islands (Supplementary Fig. S4A¬C). Single reticulated specimens in which the bars or plates have a somewhat 'beaded' appearance, probably reflecting lobated margins, were seen at Stns 6 and 10 (Dives 5 and 7) (Supplementary Fig. S4D, E). Finally, a single dark dome with paler-tipped excrescences occurred at Stn 6 (Dive 5) (Supplementary Fig. S4F).

(iii) Smooth, pale tests with relatively wide bar or plate-like elements. These are present at all sites except Stn 12 and most common at Stn 4. The simplest examples are featureless, often sinuously curved structures (Fig. 10A-C), while others are branched (Fig. 10D-F). A few specimens form quite complex domed structures that are to some extent reticulated (Fig. 10D-I). We regard the complicated, reticulated individuals as a separate morphotype, although it is possible that this rather diverse assemblage of specimens, which share the same distinctive smooth pale appearance, represents a single variable species.

3.3.2. *Collected specimens and fragments*

Xenophyophores were found in 12 samples (three box cores, seven multiple cores, two epibenthic sledge samples) from seven of the 16 sites sampled to the south of the Aleutian Islands (Table 4). Three intact specimens were recovered in cores, the others were represented by fragments. The collection included eleven forms that were fairly distinctive. The remaining fragments were considered indeterminate.

Table 4
Xenophyophores collected at stations south of the Aleutian Islands. The Roman numerals in the left-hand column refer to the brief descriptions given in the text. N = number. F = Fragment. BC = Box core. MuC – Multiple corer. EBS – epibenthic sledge.

Xenophyophore	N	Figure	Stn-deployment	Sample	Depth (m)
(i) *Reticulammina* sp.	1	11A-C	7–9	BC	6554
(i) *Reticulammina* sp.(fragments)	5F		7–6	MuC#2	6555
(ii) *Reticulammina*-like	1	11D-F	6–5	BC	5317
(iii) Plate-like fragments form 1 (thinner)	20F	12A-D	6–6	MuC#1	5316
(iv) Plate-like fragments form 2 (thicker)	5F	12E-H	6–6	MuC#1	5316
(v) Plate-like fragment form 3 (complex)	1	13A-D	10–6	BC	5098
(vi) Small intact plate	1	13E-H	8–7	MuC#2	4612
(vii) Smooth, pale, fine-grained (plate & cylindrical)	2F	14A-C;	12–5	EBS#1	4291–4305
(vii) Smooth, pale, fine-grained (plate & cylindrical)	24F	S5A-H	12–8	MuC#2	4305
(vii) Smooth, pale, fine-grained (cylindrical)	2F	14D, E	12–9	EBS#2	4302–4319
(viii) Plate-like, thin wall, spicule-rich interior	10F	15A-C	12–8	MuC#2	4305
(ix) Soft, muddy fragments, channels with stercomata	16F	15D-F	12–8	MuC#2	4305
(x) Perforated plate-like fragments	4F		12–5	EBS#1	4302–4319
(x) Perforated plate-like fragments	~100F	16	12–8	MuC#2	4305
(x) Perforated plate-like fragments	10F		12–9	EBS#2	4291–4305
(xi) Reticulated tube fragments	9F	S6	7–6	MuC#2	6555
Indet. plate-like fragments	7F		4–8	MuC#2	4640
Indet. plate-like fragment	1F		9–14	MuC#1	6500
Indet. lumpy fragment	1F		12–7	MuC#1	4304
Indet. plate-like fragment	1F		12–7	MuC#1	4304

See Appendix B for more detailed descriptions of these forms.

(i) *Reticulammina* sp. (Stn 7; Fig. 11A-C): a reticulated test with fairly thick bars merging into plate-like elements that delimit rounded open spaces.

(ii) *Reticulammina*-like (Stn 6; Fig. 11D-F): a small, irregularly reticulated test defined by curved, plate-like elements.

(iii) Plate-like fragments form 1 (Stn 6; Fig. 12A-D): very thin, and fairly flat fragments with well-defined walls and few internal particles.

(iv) Plate-like fragments form 2 (Stn 6; Fig. 12E-H): distinctly thicker and darker fragments than those of Form 1 with numerous internal mineral particles.

(v) Plate-like fragment form 3 (Stn 10; Fig. 13A-D): a single, fairly thick fragment, similar to form 2 but larger and more complicated.

(vi) Small intact plate (Stn 8; Fig. 13E-H): a single pale greyish specimen with an undulating, upturned rim.

(vii) Smooth, pale, fine-grained fragments (Stn 12; Fig. 14; Supplementary Fig. S5): A distinctive form that includes some plate-like fragments and others that are elongate and bar-shaped. All have a homogenous interior with stercomare-filled channels.

(viii) Fragments with thin wall (Stn 12; Fig. 15A-C): mainly plate-like fragments that incorporate bar-like elements and have a spicule-rich interior.

(ix) Muddy fragments with stercomare-filled channels (Stn 12; Fig. 15D-F): a collection of soft, very fragile, thick, mainly plate-like fragments.

(x) Perforated plate-like fragments (Stn 12; Fig. 16): mainly flat fragments, most of them punctuated by open spaces of different sizes and shapes.

(xi) Reticulated tube fragments (Stn 7; Supplementary Fig. S6): simple, coarse-grained tubes, mainly branched but including one that forms a complete circuit.

3.3.3. Associated organisms

A hexactinellid sponge was attached to the surface of the largest specimen (registration number SMF 1) of *Syringammina limosa* from Stn 1. We did not notice any other organisms associated with the collected xenophyophores, although we did not search systematically for such organisms. However, ophiuroids were sometimes seen in close proximity to xenophyophores in OFOS photographs (Fig. 10B, C, F, H; ASupplementary Fig. S3H, S4D).

4. Discussion

4.1. Study limitations

We obtained xenophyophores from samples on an opportunistic basis. Where possible, we examined the surfaces of box cores and multiple cores and sorted through multicorer residues for xenophyophore fragments, as well as smaller foraminifera. In the case of epibenthic sledge catches, we had access to small subsamples, but xenophyophores were not generally picked from the remainder of the sample. Our survey of collected material was therefore incomplete and largely qualitative.

The analysis of xenophyophores in images obtained during the six OFOS dives to the south of the Aleutian Islands posed some challenges. The densities (Table 2) were analysed systematically, based on 50 images, following the protocol of Sigwart et al. (2023). However, 50 frames was not sufficient to adequately assess the occurrence of different morphotypes. All or most of the OFOS images from each station were therefore examined for obvious xenophyophores but not exhaustively, hence only abundance categories rather than precise data are reported in Table 3. At particular sites, it is usually possible to distinguish several distinct forms. Some of these are rare or uncommon and were seen only in images from one dive. A few common forms have fairly consistent morphologies across sites, but other morphotypes (notably the plate-like forms) appear quite variable within and particularly between sites, making it likely that they encompass a number of species. There is also always a residue of individuals that are difficult to confidently assign, sometimes because the images are not sufficiently clear. This was a particular problem at Stn 12 (Dive 8) where, rather surprisingly, xenophyophore numbers in OFOS images were lower than at any other site, although the samples yielded the largest number of fragmentary specimens. Despite these sources of error and uncertainly, we believe that the OFOS images provide a good indication of xenophyophore diversity in this region.

4.2. Comparison of xenophyophores on either side of the Aleutian Islands

The general impression from the samples we examined is that xenophyophores are not particularly abundant at most stations to the south of the Aleutian Islands. Only a few specimens were seen on box core and multiple core surfaces. This is consistent with our quantitative counts, which show that, except for Stn 4, densities are at least an order of magnitude lower in deeper water to the south of the islands compared to the values reported by Sigwart et al. (2023) from the Bering Sea

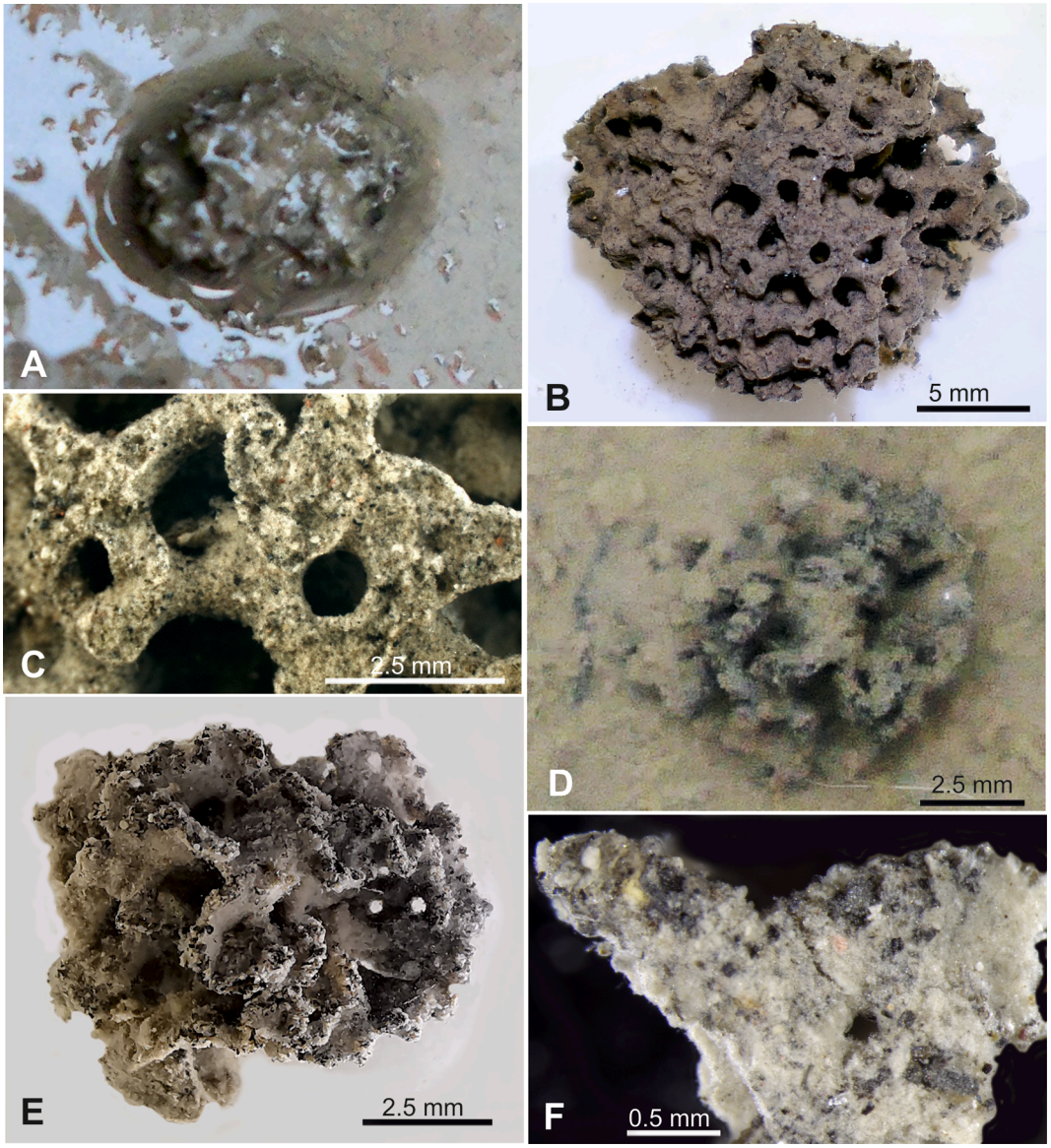

Fig. 11. (A¬C) *Reticulammina* sp., Stn 7–9, BC, shipboard photographs. (A) Specimen as first seen on box core surface. (B) Entire specimen after cleaning. (C) Detail showing test structure. (D¬F) *Reticulammina*-like, Stn 6–5, BC. (D) Specimen as first seen on box core surface. (E) Shipboard photograph of entire specimen after cleaning. (F) Detail of test fragment, photographed in Geneva. A scale is not available for (A).

(Table 2). On the other hand, the OFOS images and collected material suggest that xenophyophores are at least as diverse at these deeper sites as they are in the Bering Sea. The three or four morphotypes (?species) recognised at Stns 1–3 (water depth 3504–3652 m) compares with the sixteen forms seen at six stations along the flanks of the Aleutian trench (4612–6555 m), with an additional eight or so forms collected but not identifiable in OFOS images. This greater overall diversity must reflect the larger number of deeper stations investigated and their variation in terms of depth, sediment characteristics, bottom-water oxygen and other environmental parameters. Nevertheless, a relatively high diversity is also indicated by the number of morphotypes at particular sites; this ranges from two (Stn 12) to eight or nine (Stns 10, 4, 6), with six at Stn 14 and seven at Stn 8 (Table 3). An important caveat is that, as explained above, the numbers of morphotypes (presumed species) is only tentative.

There are some similarities between morphotypes in OFOS images to the north and south of the Aleutian Islands. Firstly, *Syringammina limosa* (identified genetically), the dominant xenophyophore species in the Bering Sea, may be present in deeper water to the south. Some of the more regularly reticulated specimens in OFOS images from the Bering Sea resemble a few reticulated domes in images from Stns 4, 8 and 10 (Dives 4, 6 and 10; 4593–5093 m) (compare Fig. 3G with Supplementary Fig. S4A¬C). There are also close similarities between the irregular individuals of *S. limosa* from the Bering Sea and domes with very narrow, jagged, irregular ridges seen in OFOS images from Stn 4 (Dive 4; 4593–4610 m) (compare Fig. 9G¬I with Fig. 3J¬L). Secondly, some of the folded, plate-like Bering Sea morphotypes (e.g., Fig. 5A¬F) resemble those in images from deeper sites (e.g., Fig. 7A¬C), while two atypical individuals seen in the Bering Sea (Fig. 5K, L) are reminiscent of one of those photographed at Stn 10 (Dive 7; 5093 m) (Fig. 7D). However, closely related species, including of *Syringammina,* can look very similar, even in laboratory or shipboard photographs (compare *S. limosa* and *S. corbicula,* as illustrated by Voltski et al., 2018; Richardson, 2001, respectively), making them difficult to distinguish in seafloor photographs. Identifications may be more secure at the genus level, however. Other morphotypes that are common at sites to the south of the Aleutian Islands are not obviously present in the Bering Sea. The pale smooth morphotypes (Fig. 10; simple/branched and reticulated forms) are seen

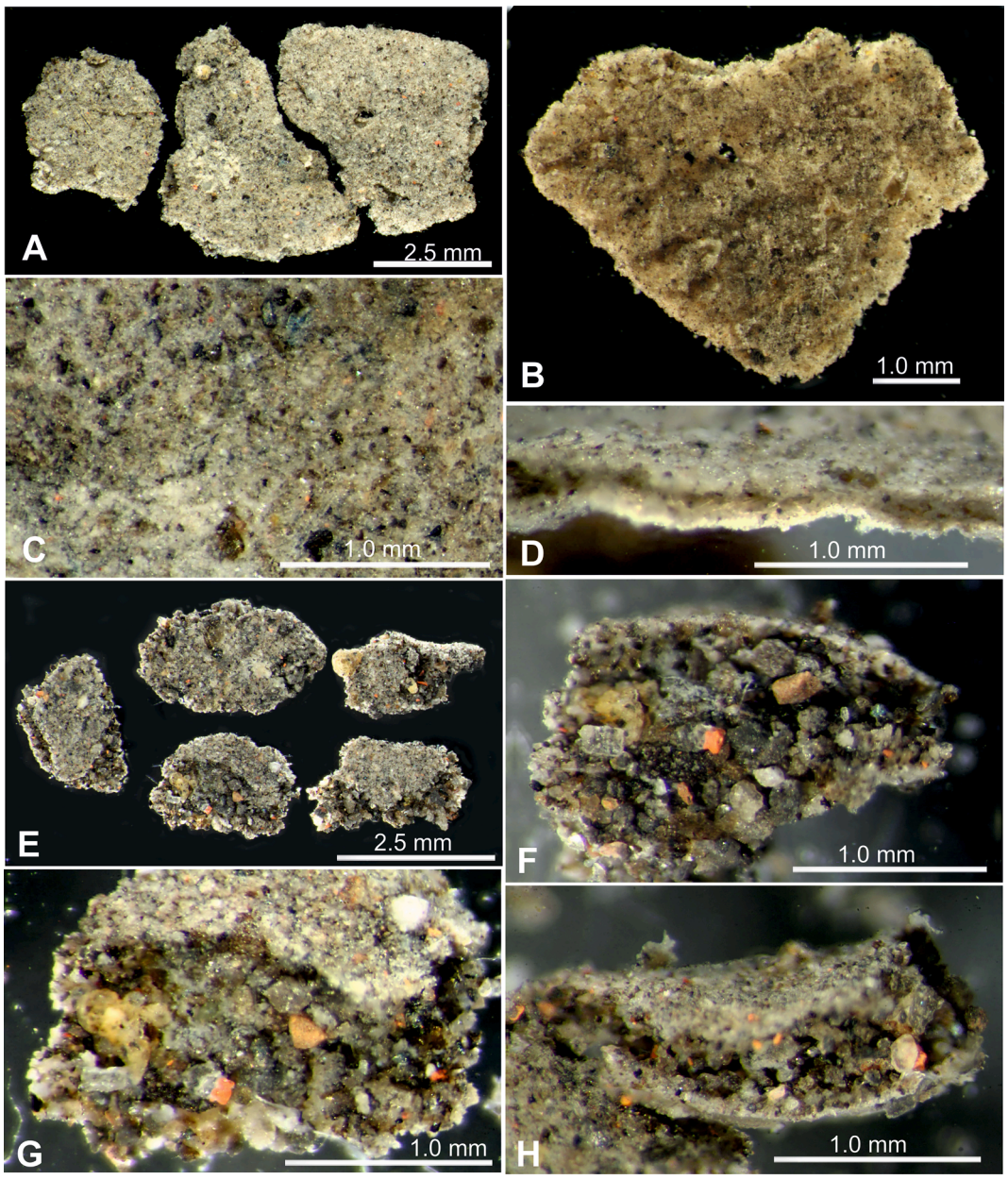

Fig. 12. Plate-like xenophyophore fragments from Stn 6–6, MuC#1, >500 μm fraction: photographed in Southampton. (A¬D) Form 1 with thin test. (A) General view of three fragments. (B) Another fragment with vague furrows. (C) Detail of outer agglutinated surface. (D) Broken edge of fragment. (E¬H) Form 2 with thicker test. (A) General view of fragments. (F¬H) Various views of broken edges showing numerous large internal mineral grains.

at all the southern sites, except Stn 12 (Dive 8), but not in the Bering Sea. Their pale surfaces make them particularly obvious in OFOS images. The finely reticulated domes, which are very common at Stn 10 (Dive 7, 5084–5093 m), constitute the other main morphotype apparently restricted to the southern sites. These two forms probably correspond to the *Reticulammina* sp. and 'Smooth pale, fine-grained fragments' (respectively, forms i and viii above) that were collected in samples. Several uncommon morphotypes are also confined to deeper sites. These include the distinctive, irregular 'spiky' form from Stns 6 and 10 (Dives 5 and 7; 5084–5327 m).

One issue that could not be addressed adequately during this study is whether xenophyophores live at hadal depths in the Aleutian trench, too deep for OFOS to be used because the fibre optic cable was not long enough. Although previous reports from extreme hadal settings (Gallo et al., 2015) show that water depth itself is no barrier to xenophyophores, none of the the AleutBio samples obtained at depths > 7000 m (four box cores, five EBS and two Agassiz trawls) yielded obvious xenophyophore remains. However, the box core samples revealed very soft sediments in the trench axis (Brandt, 2022). Possibly, these soupy sediments do not provide a sufficiently firm surface on which the xenophyophores can settle and develop, although it would impose no constraints on infaunal species (Tendal et al., 1982). Clearly, this question can only be resolved by more extensive sampling.

4.3. Possible connections between S. limosa populations in the Okhotsk and Bering seas

This species occurs at similar depths in the Bering Sea (3507–3653 m) and the Sea of Okhotsk (3351–3366 m). The geographical setting and environmental characteristics are also similar. Both are marginal seas separated from the North Pacific by a chain of volcanic islands. The two sampling sites in the Sea of Okhotsk had bottom-water oxygen

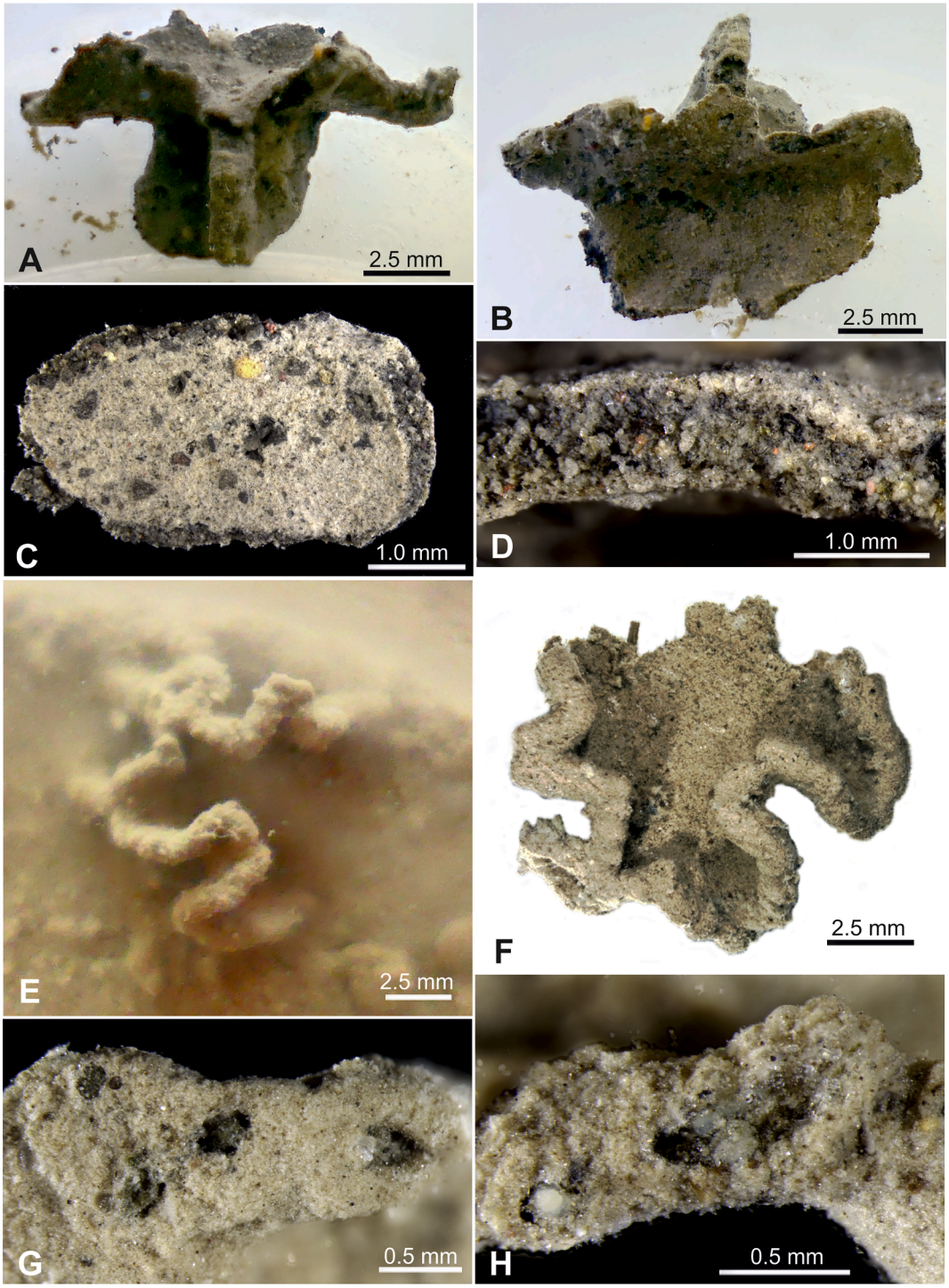

Fig. 13. (A¬D) Fragments of complex plate, Stn 10–6, BC. (A, B) Shipboard photographs showing different views of the fragment, as originally found. (C, D) Photographs taken in Geneva of smaller fragment derived from original larger fragment. (C) Entire fragment. (D) Broken edge. (E¬H) Small plate with undulating rim, Stn 8–7, MuC#2. (E) Intact plate as originally seen on core surface. (F) Shipboard photograph of more or less intact specimen. (G, H) Geneva photographs (G) Detail of damaged rim photographed showing stercomare visible through hole. (H) Another part of rim showing stercomare and pale granellare strand.

concentrations of 79.7 and 81.4 μmol/L (= 1.78 and 1.82 ml/L) and bottom-water temperatures of 1.9C (Voltski et al., 2018). The corresponding values in the Bering Sea were ~ 56.5 and ~ 58 μmol/kg (= 1.27 ml/L and 1.30 ml/L) at Stns 1 and 2, respectively, and ~ 1.6 C at both sites (Fig. 5.28 in Theising et al., 2022). Salinity values were more or less the same in both areas. Although xenophyophores are often found in well-oxygenated waters, *S. limosa* is associated with relatively low bottom-water oxygen concentrations, particularly in the Bering Sea. However, evidence from elsewhere in the Pacific Ocean suggests that xenophyophores can tolerate concentrations as low as 0.4 ml/L (Levin, 1994), so the oxygen values in these two marginal seas probably do not pose a serious constraint on *S. limosa* (see also Ashford et al., 2014).

Stn 1 is separated from the two sampling areas in the Sea of Okhotsk by distances of > 2700 km, demonstrating that *S. limosa* has a genetically confirmed range spanning a considerable distance. Ranges of this order may not be unusual among xenophyophores. Two species,

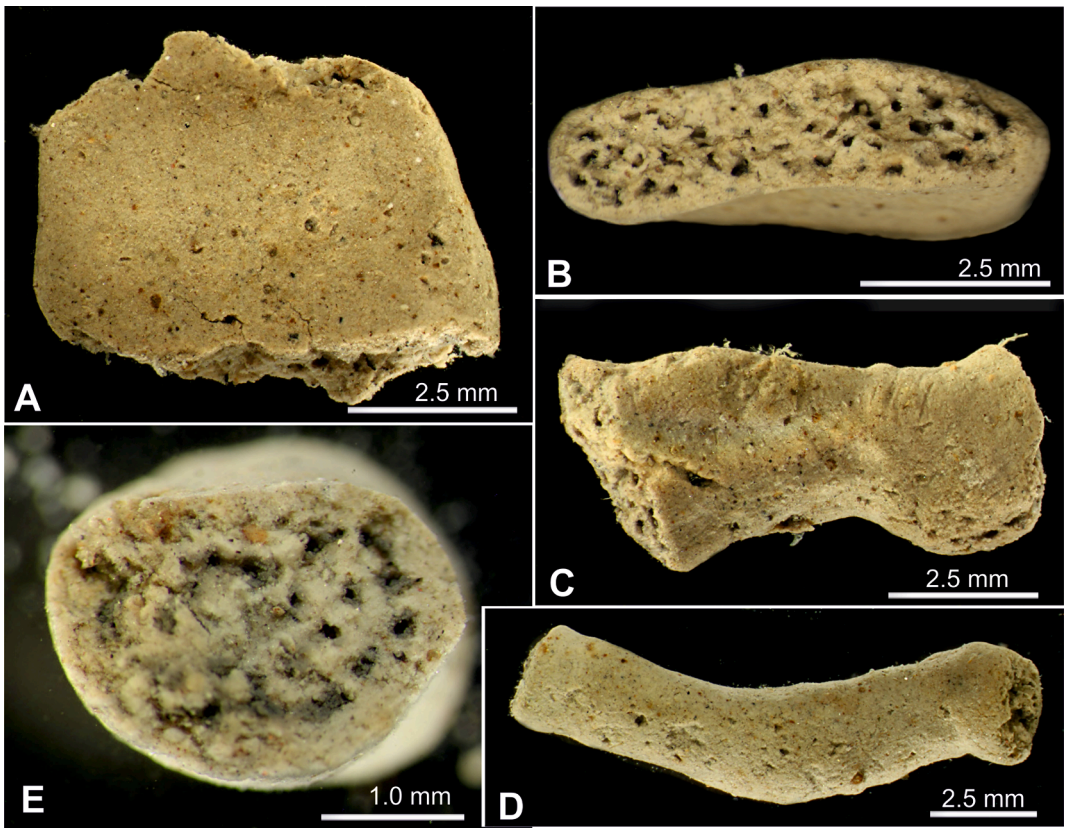

Fig. 14. Smooth, pale, fine-grained fragments photographed in Southampton. (A¬C) Stn 12–5, EBS#1. (A) Entire fragment. (B) Broken edge showing cross −sections of channels with decayed stercomare in fine-grained test interior. (C) Elongate fragment. (D, E) Elongate, cylindrical fragment, Stn 12–9, EBS#2. (D) Entire fragment. (E) Broken end showing interior penetrated by channels with stercomare.

Aschemonella monilis and *Moanammina semicircularis,* have genetically supported ranges of at least 3,800 km across the equatorial Pacific Clarion-Clipperton Zone (CCZ) (Gooday et al., 2020b). Much longer ranges have been claimed for some other species, for example, ocean-wide (>10,000 km) in the case of *Reticulammina novaezelandica* (Araya and Gooday, 2018) and global in the case of *R. labyrinthica* (Gooday and Tendal, 1988). However, these are based only on test morphology.

Although *Syringammina limosa* occurs in two semi-isolated marginal seas with no direct connection, both seas communicate hydrographically with the North Pacific via deep passages between the chains of volcanic islands that separate them from the adjacent ocean. The Okhotsk Sea is the source for North Pacific intermediate water, which flows out through the deep Bussol (maximum depth 2318 m) and Kruzenshterna (1920 m) Straits (Takahashi 1998), while deep Pacific water flows into the Sea, mainly through the Kruzenshterna Strait (Tyler, 2003). The Bering Sea is also far from being hydrographically isolated. Instead, it is strongly influenced by the inflow of Pacific water through deep channels between the Aleutian Islands, the deepest being the Kamchatka Strait (maximum depth 4420 m) (Takahashi, 1998; Khen et al., 2013).

Analyses of extensive samples collected during the SokhoBio expedition reveal that many metazoan species occur both in the Kuril Basin (the deepest part of the Okhotsk Sea), and the NW Pacific (Malyutina et al., 2018). They included some isopods, peracarid crustaceans that brood their young and have limited dispersal potential (Brandt et al., 2018). Some benthic foraminifera are believed to disperse in the form of propagules (zygotes or tiny juveniles) that can be carried by currents and will only develop further if they settle where the environmental conditions are favourable (Alve and Goldstein, 2003, 2010). Lagrangian particle tracking experiments suggest that the flow of deep water in the NW Pacific might have the potential to transport xenophyophore propagules, or possibly small test fragments, from the Okhotsk into the Bering Sea, most likely via the Kamchatka Straight at the western end of the Aleutian Islands (Kawasaki et al., 2022). The observation of large xenophyophores, tentatively identified as *Syringammina fragilissima,* in 1996 on a thick volcanic ash layer deposited 6 years earlier over large parts of the South China Sea (Hess et al., 2001) shows that xenophyophores can disperse widely and quickly. Thus, there seems to be no fundamental barrier to gene flow between the Okhotsk and Bering Seas.

4.4. Some wider comparisons

As briefly reviewed in the introduction, there is a fairly extensive body of published research on Pacific xenophyophores dating back to the 19th century. Much of this has originated from tropical latitudes. Work on Pacific xenophyophores is ongoing and a detailed discussion of wider patterns would be premature. Here, we confine ourselves to some remarks about assemblages observed in two well-studied areas, the eastern Pacific seamounts and the Clarion-Clipperton Zone.

Seventeen eastern Pacific seamounts hosted a variety of morphotypes, with two, six, four, and five different forms collected at 31°, 20°, 13°, 10° N, respectively (Levin et al., 1986; Levin and Thomas, 1988; additional photographs in Levin, 1991, 1994). Specimens were obtained across a depth range from 1239 to 3353 m on sandy sediments, and at a few deeper sites with muddy sediments, as well as on hard surfaces and in a variety of settings including caldera floors, crater rims, benches and summit plateaus. The 17 morphotypes collected by Levin and Thomas (1988) across these different settings is less than the 24 or so recognised in the present study (11 collected, 16 seen in OFOS images, of which three may also be represented among the collected specimens). However, the seamount xenophyophore diversity is undoubtedly

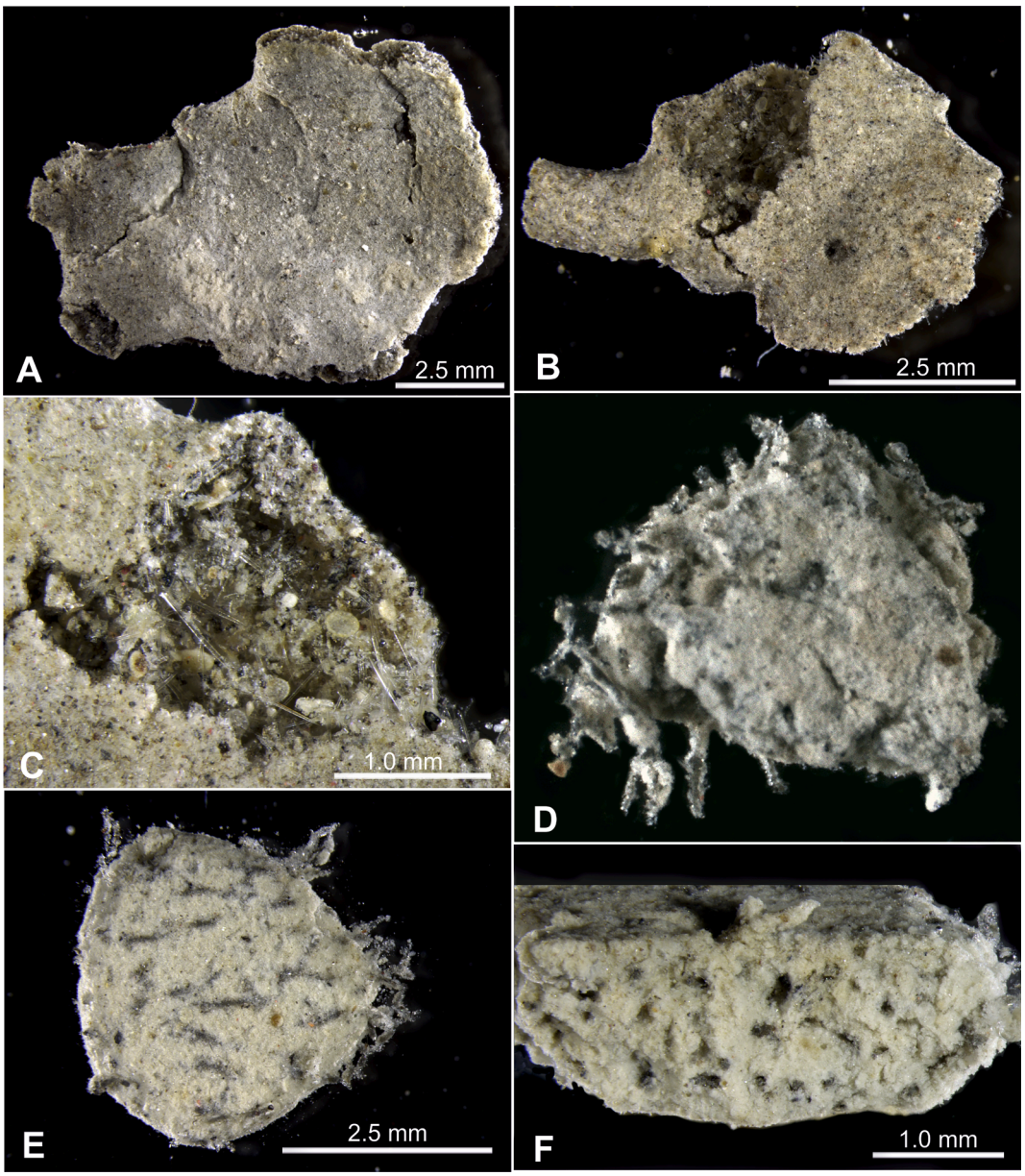

Fig. 15. Photographs taken in Geneva unless stated otherwise. (A¬C) Plate-like fragments with thin wall and spicule-rich interior. (A) Large fragment from Stn 12–7, MuC#1. (B, C) Plate-like fragment with bar-like process. (B) General view. (C) Detail showing test interior with numerous spicules. (D¬F) Fragile muddy test with stercomare-filled channel. (D) Shipboard photograph of freshly collected fragment with exposed tubes filled with decayed stercomare. (E) Preserved fragment with surface smoothed after during transport and storage showing stercomare-filled tubes exposed on surface. (F) Broken surface showing cross sections of tubes with stercomare embedded in fine-grained 'muddy' matrix. There is no scale available for D.

underestimated since additional forms were seen on the seafloor but not sampled. It seems, therefore, that the number of xenophyophore species inhabiting the two areas may be roughly similar, despite the greater degree of habitat complexity on the seamounts.

Some plate-like morphotypes from the Bering Sea (e.g., Supplementary Fig. S2A-F) are similar to a folded plate-like specimen assigned to *Psammina* from a cauldera floor at 1957 m depth on a 20° N seamount (Fig. 1C in Levin and Thomas, 1988). Reticulated forms with fairly thin, plate-like lamellae (Fig. 2a-e in Levin and Thomas, 1988) somewhat resemble our dome with sinuous, largely reticulated plates (Fig. 9D-F), although they are not similar enough to be considered the same species. Otherwise, there are few parallels between morphotypes from the two regions, perhaps reflecting the much shallower depths of many of the seamount sampling sites.

A much larger number of xenophyophores species and morphotypes has been recognised within the CCZ, a reflection partly of the vast area (4.5 million square kilometres) covered by this region. Around 70 species, either described or undescribed, have been collected (Gooday et al., 2017a, 2020a, 2024; Gooday and Wawrzyniak-Wydrowska, 2023), with additional morphotypes recognised in seafloor photographs (Kamenskaya et al., 2013; Amon et al., 2016; Simon-Lledó et al., 2019a; Simon-Lledó et al., 2019b). The Aleutian and CCZ xenophyophores have little in common. For example, the stalked *Psammina* species and *Aschemonella monilis,* which are common and dominant components, respectively, of the CCZ assemblages, are notably absent in our samples and OFOS images. This may be because they are mainly sessile and depend, like many other CCZ xenophyophores, on the presence of nodules (Table 1 in Gooday et al., 2020a). However, reticulated domes resembling our Bering Sea *Syringammina limosa* constitute a possible exception. Simon-Lledó and colleagues identified an almost identical

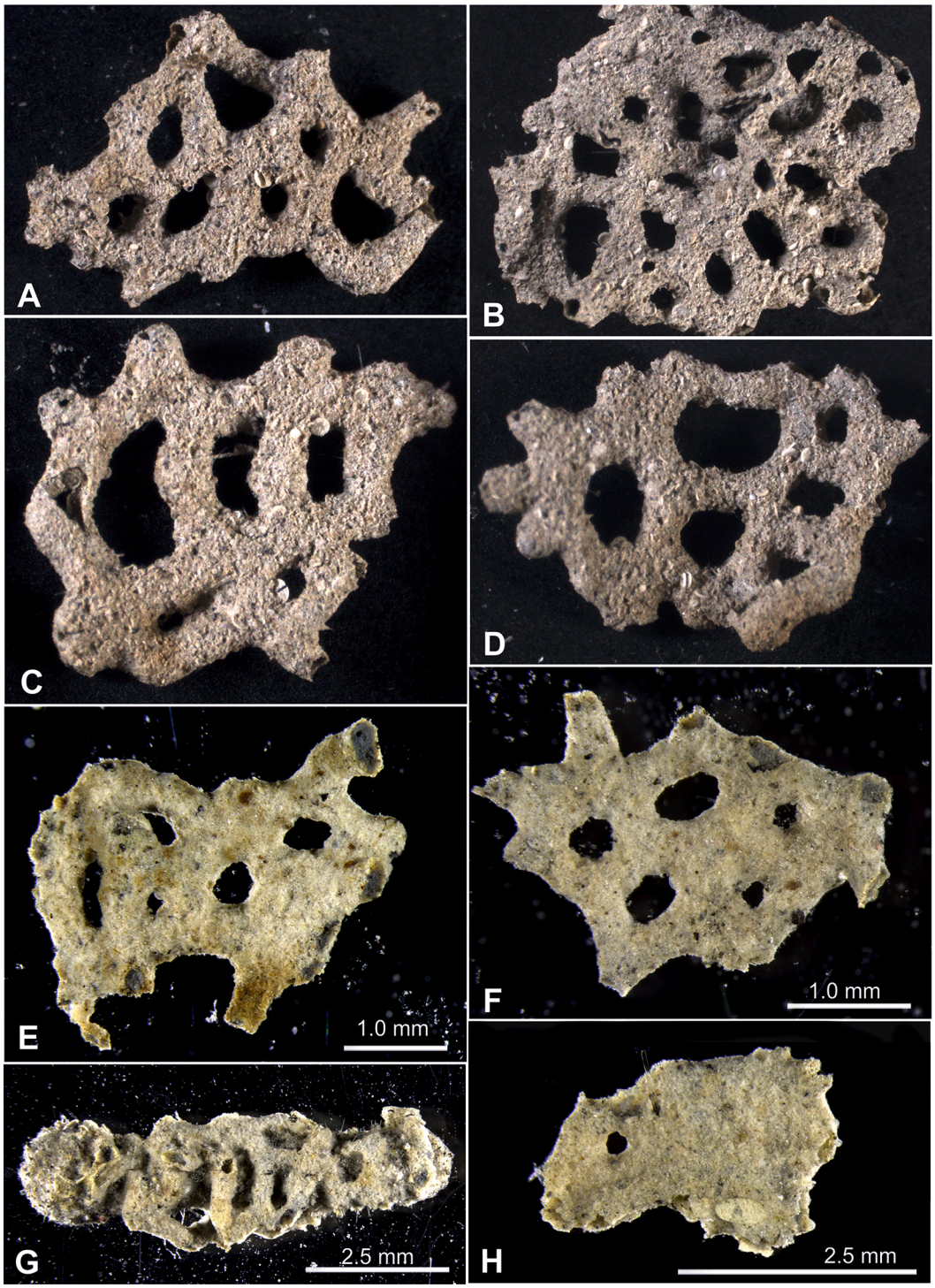

Fig. 16. Flat, perforated plate-like fragments, Stn 12–8, MuC#2. (A¬D) Shipboard photographs of dry fragments. (E¬H) Preserved fragments in water, Southampton photographs. (E, F) Typical fragments. (G) Reticulated specimen attached to agglutinated tube (*Hyperammina* sp.). (H) Plate-like fragment with single small perforation. There are no scales available for A¬D.

morphotype seen in a seabed photograph from APEI-6 as *Syringammina* cf. *limosa* and a very similar reticulated dome as 'Indeterminate Psamminid ….. possibly *Shinkaiya* or *Syringammina*' (Fig. 10e and 10d, respectively, in Simon-Lledó et al., 2019a). In a subsequent paper, Simon-Lledó et al. (2019b, Fig. 10O therein) illustrated a group of three 'reticular xenophyophores' in a photograph taken to the west of the CCZ (>5000 m depth) near the equator in the Exclusive Economic Zone (EEZ) of Kiribati. These also resemble *S. limosa,* as does a reticulated dome from APEI-7 in the western CCZ (Fig. 2A in Gooday et al., 2020a). Possibly, this species has a wide distribution in the Pacific, but confirmation requires the collection and sequencing of specimens.

Test sizes in both assemblages are typically ≤ 5 cm, generally similar to intact specimens in our study. However, three of the seamount morphotypes are considerably larger (Levin and Thomas, 1988): 'platy tests' from 10° N (12 cm); reticulated dome from 13° N (15 cm); and a *Reticulammina* species from 10° N that reportedly reached the extraordinary size of about 30 cm! There are also some larger CCZ species. These include *Abyssalia* aff. *foliformis* (5.8 cm), *Aschemonella monilis* (up

to 7 cm), *Claraclippia seminuda* (~8 cm), *Psammina* sp. B (8 cm) and *Moanammina semicircularis* (9 cm) (Gooday et al., 2017b, 2020b, 2024). In contrast, the largest xenophyophores seen in our OFOS images were 5–6 cm in size.

5. Concluding remarks

Despite its limitations, this survey of collected material and seabed (OFOS) photographs has greatly enhanced our previously sparse knowledge of xenophyophores in the northern North Pacific and Bering Sea. Interestingly, all of the xenophyophores found in our samples and recognised in seafloor images are members of the order Psamminida (sensu Tendal, 1972), whereas all of the species recorded by Tendal (1972) in samples collected during Russian *Vityaz* cruises to the north of 40°N off the Kamchatka Peninsula and in the region of the Aleutian Trench were members of the genus *Stannophyllum*, which belongs to the order Stannomida.

Four or five morphotypes, including *Syringammina limosa,* can be recognised in the OFOS images from the Bering Sea and a total of 16 in deeper water to the south of the Aleutian Islands, although not all were common. In both areas, there was limited correspondence between morphotypes seen in seafloor images and those collected. Only three of the eleven collected morphotypes from the Aleutian area (*Reticulammina* sp., 'Intact plate with undulating rim' and 'Smooth, pale, fine-grained form') could be tentatively recognised in OFOS images from the deeper sites, while another three that were morphologically distinctive ('*Reticulammina*-like', 'Flat, perforated plate-like fragments' and 'Reticulated tube') were not obviously represented in the images; the latter two may be infaunal. The other five forms were too fragmented for any comparison to be attempted. Our observations therefore indicate that at least 24 xenophyophore morphotypes (morphospecies?) live at abyssal depths on the flanks of the Aleutian Trench. The seafloor images suggest that some morphotypes, including those resembling *S. limosa,* may be present in the Bering Sea and at deeper water sites to the south of the Aleutian Islands, although this requires confirmation.

The samples and particularly the OFOS images obtained during the AleutBio cruise provide a first glimpse of the diversity and distribution of xenophyophores in a region where these giant foraminifera were previously poorly known. The minimum of 24 morphotypes in the Aleutian Trench area and four in the Barent Sea is much less than the 70 or so currently recorded from the CCZ and further sampling will undoubtedly reveal more. Clearly, there is much to learn. Seafloor imagery gives an overview the xenophyophores present in an area, but it is not always easy to consistently distinguish morphotypes or to link them to physical collections. More specimens in good condition, together with molecular data, will be required in order to better document xenophyophore diversity and distribution in the Bering Sea and northern North Pacific.

CRediT authorship contribution statement

Andrew J. Gooday: Writing – review & editing, Writing – original draft, Visualization, Methodology, Investigation, Formal analysis, Data curation, Conceptualization. **Maria Holzmann:** Writing – review & editing, Writing – original draft, Validation, Methodology, Funding acquisition, Formal analysis, Data curation. **Jan Pawlowski:** Writing – review & editing, Methodology.

6. Data availability

DNA sequences for *Syringammina limosa* are deposited in Genbank. All other data generated and analysed during this study are included in this published article. Collected specimens of *Syringammina limosa* are housed in the collections of the Naturmuseum Senckenberg, Frankfurt, Germany with the following registration numbers Collection Foraminifera marin rezent – SMF 1¬4. Other material is stored in the authors' collection in Geneva and Southampton and can be inspected on reasonable request.

Declaration of competing interest

The authors declare that they have no known competing financial interests or personal relationships that could have appeared to influence the work reported in this paper.

Acknowledgements

This work is a product of the "AleutBio" expedition onboard R/V SONNE (cruise SO293). We thank Prof. Dr Angelika Brandt for inviting two of us (AJG, JP) to participate in the AleutBio project and scientists on the cruise for their help and support, particularly Dr Karin Meissner and the box core team, Dr Davide De Franco, Karen Jeskulke and the epibenthic sledge team, Freddie Bonk and the multicore team. We are particularly grateful to Drs Chong Chen and Anna Jażdżewska, who photographed some of the xenophyophores for us, and Dr Jennifer Durden who provided advice on image analysis. The support from the Master and crew of the SONNE during deployments of OFOS and sampling gears is also gratefully acknowledged. We thank two anonymous reviewers for their helpful comments that substantially improved the manuscript. MH acknowledges support from the Schmidheiny foundation, under a grant entitled 'Exploring abyssal and hadal biodiversity of foraminifera in the North Pacific'. This is AleutBio publication #13.

Appendix A

Here we give fuller descriptions of the eleven forms recognised in collected samples and summarised in Section 3.2.2.

Plate-like Form 1 (Fig. 6A, B). Two small fragments from a multicore are 2.8 and 4.0 mm in maximum dimension and basically plate-like but variable in thickness (0.7–1.4 mm). The wall is thin (35–50 μm), well-defined, rather soft and composed mainly of mineral grains with scattered diatoms. It is generally fine-grained, although the grains are of different sizes and of different types, including some that are orange in colour. The test interior contains the grey, powdery remains of decayed stercomare mixed with diatoms.

Plate-like Form 2 (Fig. 6C, D). The EBS sample from Stn 1 yielded a number of pale, plate-like fragments that are clearly different from Form 1. The largest of these, measuring 7.95 x 3.86 mm, had split along the plane of the plate (Fig. 6C, D). One side shows the outer surface, which is fairly smooth, light grey, finely agglutinated but with a scattering of centric diatom frustules. The other side, which shows the test interior, is covered by numerous diatoms that are woven together with branching stercomare strands, typically 65 to 110 μm wide.

Bar-like Form 3 (Fig. 6E-H). A single fragment from the Stn 1 EBS sample is subcylindrical, measuring 6.2 mm long and 2.5 mm wide, expanding to 3.2 mm at the intact end and flattened in cross section (Fig. 6E, F). The surface is pale grey, generally smooth and fine-grained but incorporates a scattering of centric diatom frustules, some of which project at an angle from the surface. The broken end shows an outer zone, 330–500 μm thick, enclosing the test interior in which the agglutinated material is punctuated by channels, mostly seen as oblique cross sections. Three small irregularly shaped fragments from MuC #1 (Stn 1), the largest measuring only ~ 2.6 mm maximum dimension, may represent the same form (Fig. 6G, H). They are composed of soft, fine, whitish material incorporating occasional diatom frustules. The composition is homogeneous with no distinct surface layer and the interior is ramified by stercomare strands that are almost black and contain well-preserved stercomata. They run roughly longitudinally and some end blindly.

Appendix B

Here we give fuller descriptions of the eleven forms recognised in collected samples and summarised in Section 3.3.2.

(i) *Reticulammina* sp. (Fig. 11A-C).

The largely intact test and picked from the box core surface (Stn 7) and some fragments that may represent the same species were found in MuC#2 from the same station. The intact specimen has a reticulated test, measuring around 20 x 17 mm, comprising fairly thick bars merging into plate-like elements delimiting rounded open spaces. There is a thin, fairly fine-grained surface layer beneath which the test interior is filled with mineral grains in a fine-grained matrix (Fig. 11C). The single specimen is probably the same as the finely reticulated form that is common in the OFOS images from Stn 7 (Fig. 9A-C). It is quite similar to *Reticulammina novaezealandica,* described by Tendal (1972) from much shallower depths (743–984 m) off New Zealand, but the internal xenophyae are mineral grains rather than foraminiferan tests.

(ii) *Reticulammina*-like (Fig. 11D-F).

This small, roughly dome-like test, measuring 8.3 x 5.9 x 3.3 mm, was also found largely intact on a box core surface (Stn 6). The irregularly reticulated structure is defined by curved, plate-like elements. Some areas of the surface are relatively smooth, predominantly fine-grained and light grey in colour but other parts are encrusted with large, dark grains together with a few diatoms and sponge spicule fragments. The wall is thin and because it includes these large grains, the interior space is irregular in width. It contains stercomare with fresh stercomata and a few possible pale whitish granellare branches, ~25 to 30 μm in diameter.

(iii) Plate-like fragments form 1 (Fig. 12A-D).

Numerous fragments were found in MuC#1 (Stn 6). They are irregularly shaped, fairly flat and thin. The largest pieces measure 3.1 x 5.4 mm with a thickness of 0.23 to 0.38 mm. The wall is very thin (~35 to 50 μm), fairly coarse-grained with a rather rough outer surface, comprising a mixture of mineral grains of different sizes and types as well as sponge spicules, some of which project into the test interior. The plate-like morphology suggests a placement in *Psammina.* However, the wall is continuous around intact parts of the margin with no obvious apertures. There is no evidence of internal partitions or pillars on broken edges.

(iv) Plate-like fragments form 2 (Fig. 12E-H).

The same multicorer sample (MuC#1, Stn 6) yielded a number of thicker and plate-like fragments, measuring up to 2.3 x 3.0 mm and ~ 0.45 to 0.67 mm thick. The wall is dark grey, very thin (~30–40 μm), coarse grained and composed of mineral grains of different sizes, some almost black and other lighter greyish or whitish, in addition to a scattering of small orange particles. The test interior is occupied by a jumble of large mineral grains between which stercomare masses are sometimes visible. Saidova (1970) described *Astrorhizinella planata,* a rather similar plate-like species with a similar thickness (0.4 to 0.7 mm). This was transferred to *Psammina* by Tendal (1996) and redescribed by Kamenskaya and Saidova (1998). However, Saidova's species was from two much deeper sites (6835 and 7295 m depth) in the Kamchatka Trench, and the identification cannot be confirmed.

(v) Plate-like fragment form 3 (Fig. 13 A-D).

This complicated fragment, ~12.5 mm maximum dimension, was found on the surface of the Stn 10 box core. It comprises a larger plate curving through almost 90° with a side plate (perforated by an open space) arising from the centre of the convex side and dividing into two smaller plates. The thin (~60¬90 μm) surface layer is light greyish, delicate, and fine grained (most particles < 10 μm), speckled with tiny dark particles and with a scattering of larger mineral grains. The interior of the plate is dark and occupied by decayed stercomare and numerous relatively large mineral grains.

(vi) Small intact plate (Fig. 13E-H).

This small plate-like specimen from the Stn 8 box core measures 10.4 x 9.0 mm and appears intact. The central part is relatively flat, but most of the outer part is raised up into a series of distinct marginal folds. A pair of lobate projections extend from the margin where these raised folds are absent. The test wall is very soft with a poorly-defined, rather flocculent, very fine-grained surface and a scattering of larger embedded particles. Broken edges show a relatively thick wall with a hollow interior containing fresh stercomare and at least one pale whitish granellare strand, ~100 μm diameter. The specimen is rather similar to one photographed by OFOS (Fig. 8J), although that was from Stn 6 (Dive 5) rather than Stn 8 (Dive 6).

(vii) Smooth, pale, fine-grained fragments (Fig. 14; Supplementary Fig. S5).

This interesting form from Stn 12 is represented in the two EBS samples and MuC#2. The EBS samples yielded a plate-like fragment, 5.4 mm long, 4.4 mm wide and 1.5–2.0 mm thick, and two more or less cylindrical fragments, one ~7 mm long, 2.5¬3.3 mm wide and the other, which is more smoothly cylindrical, 11.5 mm long and 2.2¬2.6 mm wide (Fig. 14). The test surface is pale, soft, very smooth and fine-grained except for a few relatively large brownish grains. The test interior of all fragments has a homogenous composition, similar to that of the surface. An outer zone, 225–380 μm thick in one specimen, 100–300 μm in another, encloses the inner part, which is pierced by prominent channels occupied by the remnants of stercomare. The channels are ~ 125 to 325 μm in diameter, circular to oval in shape but sometimes merging to some extent to form a more obviously labyrinthic network.

MuC#2 yielded ~ 24 fragments, most of them either bar-like or thick plate-like pieces. The plate-like fragment illustrated in Supplementary Fig. S5A¬C measures 5.41 x 4.48 mm and is 1.25¬1.46 mm thick. One end is raised into adjoining hemispherical lobes. Two cylindrical fragments measure 5.00 mm and 3.91 mm long and 2.59¬2.75 mm and 1.68¬1.89 mm wide, respectively (Supplementary Fig. S5D-H). The intact end of one of the cylindrical fragments is rounded and closed. The internal structure of plate-like and cylindrical fragments is similar to that of the EBS fragments, with a labyrinthic system of channels filled with decayed stercomare occupying the interior, which is enclosed by a featureless outer zone. In comparison with the EBS fragments, the outer surfaces of the MuC#2 fragments appear rather darker and more heterogeneous, a result of being speckled with small dark particles.

The plate-like and cylindrical fragments probably represent the same species. Although the shapes are different, they share the same test composition and have similar distinctive internal structures. It is tempting to link the plate-like fragments, in particular, with the pale, smooth morphotypes that are common in some of the OFOS images (Fig. 10). This is not consistent, however, with the fact that the fragments were found only at Stn 12 (Dive 8) where xenophyophore densities were lowest and smooth pale forms entirely absent in the seabed images. They are somewhat similar to Form 2 from the Bering Sea, but are pale tan rather than whitish with a distinctly smooth outer surface devoid of diatoms, and more densely-packed stercomare strands, as seen in broken cross sections.

(viii) Plate-like fragments with thin wall and spicule-rich interior (Fig. 15A-C).

A single relatively large fragment came from MuC#1 (Stn 12). It is plate-like, 10.8 mm long and 8.2 mm wide. The surface is interrupted by arcuate fractures that resemble the boundaries between growth zones but extend only part of the way across the fragment. Intact parts of the margin are devoid of obvious apertures. At the narrower end a rounded broken surface suggest that the fragment originally extended into a bar. MuC#2 (Stn 12) yielded about 10 fragments of various shapes and sizes. The largest measures 6.6 x 4.4 mm and includes a bar that arises from a plate-like part (Fig. 15B), another is basically bar-shaped, while other fragments are predominately plate-like. The test wall is very thin, typically only 10¬20 μm thick, fine-grained but noticeably granular, and mainly greyish although flecked with dark particles. In one fragment the wall includes numerous spicules, some protruding from the test surface. A distinctive feature of all these fragments is that the test interior is partly occupied by a mesh of sponge spicules, to which are attached

centric diatoms and mineral grains, many of them dark (Fig. 15C). All fragments are dead.

(ix) Muddy fragments with stercomare-filled channels (Fig. 15D¬F).

MuC#2 (Stn. 12) yielded about 16 fragments of this soft, very fragile form. Their basic morphology is plate-like but the plates are fairly thick, 1.10¬1.44 mm in those that were measured. They comprise an undifferentiated (solid), very fine-grained, 'muddy' matrix that is ramified by channels filled with stercomare. The channels are around 80 to 120 μm wide and surrounded by a thin layer that appears to be mainly organic. This basal layer forms tubes filled with decayed stercomare that are exposed along the edges of fragments and other areas where the muddy matrix has been eroded, possibly when the sediment was sieved in preparation for sorting. The tubes are often rather sparkly, indicating the presence of small reflective mineral grains adhering to their surfaces. There is no sign of granellare strands (cytoplasm) and the fragments appear to be dead.

(x) Perforated plate-like fragments (Fig. 16).

Numerous distinctive fragments of this form were also picked from MuC#2 (Stn 12). They were not seen on the core surface and were probably infaunal within the top 1-cm or so of the sediment. Fragments range from being more or less flat to more three dimensional and best described as plates that are perforated by open spaces with shapes varying from more or less circular to elongated slits and a wide range of maximum dimensions, from ~ 100 to 780 μm (typically 220¬540 μm). However, the open spaces sometimes dominate to the extent that the fragments resemble reticulated tubes. In some fragments of this type, short lobate processes project along undamaged sections of the margin. At the other extreme, two fragments form plates with only a single small perforation (Fig. 16H). There is also one specimen consisting of a reticulated tube that wraps around the agglutinated test of a large *Hyperammina* sp. (Fig. 16G). The test wall is greyish and composed largely of mineral grains with a sprinkling of diatom frustules. The granularity of the wall is best seen in dried fragments (Fig. 16 A¬D) and is less obvious when fragments are immersed in fluid (Fig. 16E¬H).

(xi) Reticulated tube fragments (Supplementary Fig. S6).

Nine tubular fragments measuring up to 6.5 mm in maximum extent and 0.60–1.45 mm (usually 0.80–1.0 mm) in width, were picked from MuC#2 (Stn 7). Most were branched and one formed a complete circuit around an open space, suggesting that they were part of a fragile reticulated structure, perhaps similar to the polygonal fragments of an infaunal xenophyophore from the Japan Trench (6440 m), illustrated by Swinbanks (1982). Several short branches have intact, closed ends. The wall is fairly coarsely agglutinated from mineral grains, thin (about 70–110 μm), and lacks any sign of the longitudinal internal ridges characteristic of *Occultammina* (Tendal et al., 1982). This form differs from the perforated plate-like fragments in being more clearly tubular. It may be a shallow infaunal species, like the reticulated tubes of Swinbanks (1982) and the previous species.

Supplementary data

Supplementary data to this article can be found online at https://doi.org/10.1016/j.pocean.2024.103411.

Data availability

Data will be made available on request.

References

Alve, E., Goldstein, S.T., 2003. Propagule transport as a key method of dispersal in benthic foraminifera (Protista). Limnol. Oceanogr. 48, 2163–2170. https://doi.org/10.4319/lo.2003.48.6.2163.

Alve, E., Goldstein, S.T., 2010. Dispersal, survival and delayed growth of benthic foraminiferal propagules. J. Sea Res. 63, 36–51. https://doi.org/10.1016/j.seares.2009.09.003.

Amon, D.J., Ziegler, A., Dahlgren, T., Glover, A.G., Goineau, A., Gooday, A.J., Wiklund, H., Smith, C.R., 2016. Insights into the abundance and diversity of abyssal megafauna in a polymetallic-nodule region in the eastern Clarion-Clipperton Zone. Sci. Rep. 6, 30492. https://doi.org/10.1038/srep30492.

Araya, J.F., Gooday, A.J., 2018. First record of a xenophyophore (Rhizaria: Foraminifera) on the Chilean Margin. Zootaxa 4455, 589–592. https://doi.org/10.11646/zootaxa.4455.3.16.

Ashford, O.S., Davies, A.J., Jones, D.O.B., 2014. Deep-sea benthic megafaunal habitat suitability modelling: a global-scale maximum entropy model for xenophyophores. Deep Sea Res. I 94, 31–44. https://doi.org/10.1016/j.dsr.2014.07.012.

Brandt, A., Alalykina, I., Fukumori, H., Golovan, O., Kniesz, K., Lavrenteva, A.N., Lörz, A.-N., Malyutina, M.E., Philipps-Bussau, K., Stransky, B., 2018. First insights into macrofaunal composition from the SokhoBio expedition (Sea of Okhotsk, Bussol Strait and northern slope of the Kuril-Kamchatka Trench). Deep-Sea Res. II 154, 106–120. https://doi.org/10.1016/j.dsr2.2018.05.022.

Brandt, A., 2022. SO293 AleutBio (Aleutian Trench Biodiversity Studies) Cruise Report/Fahrtbericht, Cruise No. SO293, 24.07.2022 - 06.09.2022, Dutch Harbor (USA) - Vancouver (Canada). SONNE-Berichte SO293, Begutachtungspanel Forschungsschiffe, Bonne, pp. 1-209/.

Gallo, N.D., Cameron, J., Hardy, K., Freyer, P., Bartlett, D.H., Levin, L.A., 2015. Submersible- and lander-observed community patterns in the Mariana and New Britain trenches: Influence of productivity and depth on epibenthic and scavenging communities. Deep-Sea Res. I 99, 119–133. https://doi.org/10.1016/j.dsr.2014.12.012.

Gooday, A.J., Holzmann, M., Caulle, C., Goineau, A., Kamenskaya, O.E., Weber, A.A.-T., Pawlowski, J., 2017a. Giant foraminifera (xenophyophores) are exceptionally diverse in parts of the abyssal eastern Pacific where seabed mining is likely to occur. Biol. Conserv. 207, 106–116. https://doi.org/10.1016/j.protis.2018.09.003.

Gooday, A.J., Holzmann, M., Caulle, C., Goineau, A., Jones, D.O.B., Kamenskaya, O.E., Simon-Lledo, E., Weber, A.A.-T., Pawlowski, J., 2017b. New species of the xenophyophore genus *Aschemonella* (Rhizaria, Foraminifera) from areas of the abyssal eastern Pacific licensed for polymetallic nodule exploration. Zool. J. Linn. Soc. 182, 479–499. https://doi.org/10.1093/zoolinnean/zlx052.

Gooday, A.J., Holzmann, M., Caulle, C., Goineau, A., Pearce, R.B., Voltski, I., Weber, A.A.-T, Pawlowski, J., 2017c. Five new species and two new genera of xenophyophores (Foraminifera: Rhizaria) from part of the abyssal equatorial Pacific licensed for polymetallic nodule exploration. Zool. J. Linn. Soc. 183, 723–748. https://doi.org/10.1093/zoolinnean/zlx093.

Gooday, A.J., Holzmann, M., Goineau, A., Kamenskaya, O., Melnik, V.F., Pearce, R.B., Weber, A.A.-T., Pawlowski, J., 2018. Xenophyophores (Rhizaria, Foraminifera) from the Eastern Clarion-Clipperton Zone (equatorial Pacific): the genus *Psammina*. Protist 169, 926–957. https://doi.org/10.1016/j.protis.2018.09.003.

Gooday, A.J., Durden, J.M., Smith, C.R., 2020a. Giant, highly diverse protists in the abyssal Pacific: vulnerability to impacts from seabed mining and potential for recovery. Commun. Integr. Biol. 13, 189–197. https://doi.org/10.1080/19420889.2020.1843818.

Gooday, A.J., Durden, J.M., Holzmann, M., Pawlowski, J., Smith, C.R., 2020b. Xenophyophores (Rhizaria, Foraminifera), including four new species and two new genera, from the western Clarion-Clipperton Zone (abyssal equatorial Pacific). Eur. J. Protistol. 75, 125715. https://doi.org/10.1016/j.ejop.2020.125715.

Gooday, A.J., Tendal, O.S., 1988. New xenophyophores from the bathyal and abyssal northeast Atlantic. J. Nat. Hist. 22, 413–434. https://doi.org/10.1080/00222938800770301.

Gooday, A.J., Wawrzyniak-Wydrowska, B., 2023. Macrofauna-sized foraminifera in epibenthic sledge samples from five areas in the eastern Clarion-Clipperton Zone (equatorial Pacific). Front. Mar. Sci. 9, 1059616. https://doi.org/10.3389/fmars.2022.1059616.

Gooday, A.J., Holzmann, M., Barrenechea-Angeles, M., Lim, S.-C., Pawlowski, J., 2024. New xenophyophores (Foraminifera, Monothalamea) from the eastern Clarion-Clipperton Zone (equatorial Pacific). Zootaxa 5419, 151–188.

Gouy, M., Guindon, S., Gascuel, O., 2010. SeaView version 4: a multiplatform graphical user interface for sequence alignment and phylogenetic tree building. Mol. Biol. Evol. 27, 221–224. DOI: 10.1093/molbev/msp259.

Guindon, S., Dufayard, J.F., Lefort, V., Anisimova, M., Hordijk, W., Gascuel, O., 2010. New algorithms and methods to estimate maximum-likelihood phylogenies: assessing the performance of PhyML 3.0. Syst. Biol. 59, 307–321. https://doi.org/10.1093/sysbio/syq010.

Hess, S., Kuhnt, W., Hill, S., Kaminski, M.A., Holbourn, A., de Leon, M., 2001. Monitoring the recolonization of the Mt. Pinatubo 1991 ash layer by benthic foraminifera. Mar. Micropaleontol. 43, 119–142. https://doi.org/10.1016/S0377-8398(01)00025-1.

Holzmann, M., 2024. Isolation, DNA extraction, amplification and gel electrophoresis of single-celled nonmarine foraminifera (Rhizaria). In: Practical Handbook on Soil Protists (eds.: Amaresan N., Chandarana K.A.), 181-188. 10.1007/978-1-0716-3750-0.

Hori, S., Tsuchiya, M., Nishi, S., Arai, W., Yoshida, T., Takami, H., 2013. Active bacterial flora surrounding foraminifera (Xenophyophorea) living on the deep seafloor. Biosci Biotechnol. Biochem. 77, 381–384. https://doi.org/10.1271/bbb.120663.

Kamenskaya, O.E., 2005. *Spiculammina delicata* gen. et sp. n., a new xenophyophore from the eastern Pacific (Psamminidae). Invert. Zool. 2 (1), 23–27.

Kamenskaya, O.E., Saidova, K.M., 1998. Redescription of *Psammina planata* (Saidova, 1970), a hadal xenophyophore from the Kurile-Kamchatka Trench. In: Kuznetsov, A. P., Zezina, O.N. (Eds.), Benthos of the High Latitude Regions. VNIRO Publishing House, Moscow, pp. 125–128.

Kamenskaya, O.E., Melnik, V.F., Gooday, A.J., 2013. Giant protists (xenophyophores and komokiaceans) from the Clarion-Clipperton ferromanganese nodule field (Eastern Pacific) Biol. Bull. Rev. 3 (5), 388–398.

Kamenskaya, O.E., Gooday, A.J., Tendal, O.S., Melnik, V.F., 2015. Xenophyophores (Protista, Foraminifera) from the Clarion-Clipperton Fracture Zone with description of three new species. Mar. Biodiv. 45, 581–593. https://doi.org/10.1007/s12526-015-0330-z.

Kamenskaya, O.E., Gooday, A.J., Tendal, O.S., Melnik, V.F., 2017. Xenophyophores (Rhizaria, Foraminifera) from the Russian license area of the Clarion-Clipperton Zone (eastern equatorial Pacific), with the description of three new species. Mar. Biodiv. 47, 299–306. https://doi.org/10.1007/s12526-016-0595-x.

Kaufmann, R.S., Wakefield, W.W., Genin, A., 1989. Distribution of epibenthic megafauna and lebensspuren on two central North Pacific seamounts. Deep-Sea Res. 36, 1863–1896. https://doi.org/10.1016/0198-0149(89)90116-7.

Kawasaki, T., Matsumura, Y., Hasumi, H., 2022. Deep water pathways in the North Pacific Ocean revealed by Lagrangian particle tracking. Sci. Rep. 12, 6238. https://doi.org/10.1038/s41598-022-10080-8.

Khen, G.V., Basyuk, E.O., Vanin, N.S., Matveev, V.I., 2013. Hydrography and biological resources in the western Bering Sea. Deep Sea Res. II 94, 106–120. https://doi.org/10.1016/j.dsr2.2013.03.034.

Lecroq, B., Gooday, A.J., Tsuchiya, M., Pawlowski, J., 2009. A new genus of xenophyophores (Foraminifera) from Japan Trench: morphological description, molecular phylogeny and elemental analysis. Zool. J. Linn. Soc. Lond. 156, 455–464.

Lefort, V., Longueville, J.E., Gascuel, O., 2017. SMS: Smart Model Selection in PhyML. Mol. Biol. Evol. 34, 2422–2424. DOI:10.1093/molbev/msx149.

Levin, L.A., 1991. Interactions between metazoans and large, agglutinated protozoans: Implications for the community structure of deep-sea benthos. Am. Zool. 31, 886–900.

Levin, L.A., 1994. Paleoecology and ecology of xenophyophores. Palaios 9, 32–41. https://doi.org/10.2307/3515076.

Levin, L.A., Thomas, C.L., 1988. The ecology of xenophyophores (Protista) on eastern Pacific seamounts. Deep-Sea Res. 35, 2003–2027. https://doi.org/10.1016/0198-0149(88)90122-7.

Levin, L.A., DeMaster, D.J., McCann, L.D., Thomas, C.L., 1986. Effects of giant protozoans (Class: Xenophyophorea) on deep-seamount benthos. Mar. Ecol. Prog. Ser. 29, 99–104. https://doi.org/10.3354/meps029099.

Levin, L.A., Gooday, A.J., James, D.W., 2001. Dressed up for the deep: agglutinated protists adorn an irregular urchin. J. Mar. Biol. Ass. U.K. 81, 881–882.

Malyutina, M.V., Chernyshev, A.V., Brandt, A., 2018. Introduction to the SokhoBio (Sea of Okhotsk Biodiversity Studies) expedition 2015. Deep Sea Res. II 154, 1–9. https://doi.org/10.1016/j.dsr2.2018.08.012.

Pawlowski, J., Holzmann, M., 2014. A plea for DNA barcoding of foraminifera. J. Foram. Res. 44, 62–67. https://doi.org/10.2113/gsjfr.44.1.62.

Purser, A., Marcon, Y., Dreutter, S., Hoge, U., Sablotny, B., Hehemann, Lemburg, J., Dorschel, Biebow, H., Boetius, A., 2019. Ocean Floor Observation and Bathymetry System (OFOBS): a new towed camera/sonar system for deep-sea habitat surveys. IEEE J. Ocean. Eng. 44, 87-99. DOI 10.1109/JOE.2018.2794095.

Richardson, S.L., 2001. *Syringammina corbicula* sp. nov. (Xenophyophorea) from the Cape Verde Plateau. E. Atlantic. J. Foram. Res. 31, 201–209. https://doi.org/10.2113/31.3.201.

Sagalevich, A.M., Torokhov, P.V., Matveyenkov, V.V., Galkin, S.V., Moskalev, L.I., 1992. Hydrothermal manifestations at Piyp Submarine Volcano, Bering Sea. Int. Geol. Rev. 34, 1200–1209. https://doi.org/10.1080/00206819209465662.

Saidova, K.M., 1970. Benthic foraminifera of the Kurile-Kamchatka Trench (based on the data of the 39th cruise of the R/V "Vityaz."). Trudy Instituta Okeanologii. 86, 134–161.

Saidova, K.M., 1975. Benthonic Foraminifera of the Pacific Ocean. Moskva: Academy of Sciences of the USSR, Akademia Nauk, SSSR. Instituta Okeanologii 1–875 in Russian.

Sigwart, J.D., Brandt, A., Di Franco, D., Escobar Briones, E., Gerken, S., Gooday, A.J., Grimes, C.J., Gluchowska, K., Hoffmann, S., Jażdżewska, A.M., Kamyab, E., Kelch, A., Knauber, H., Kohlenbach, K., Miguez-Salas, O., Moreau, C., Ogawa, A., Poliseno, A., Santín Muriel, A., Tandberg, A.H.S., Theising, F.I., Walter, T., Wölfl, A.-C., Chen, C., 2023. Heterogeneity on the abyssal plains: A case study in the Bering Sea. Front. Mar. Sci. 9, 1037482. https://doi.org/10.3389/fmars.2022.1037482.

Simon-Lledó, E., Bett, B.J., Huvenne, V.A.I., Schoening, T., Benoist, N.M.A., Jeffreys, R. M., Durden, J.M., Jones, D.O.B., 2019a. Megafaunal variation in the abyssal landscape of the Clarion-Clipperton Zone. Prog. Oceanogr. 170, 119–133. https://doi.org/10.1016/j.pocean.2018.11.003.

Simon-Lledó, E., Thompson, S., Yool, A., Flynn, A., Pomee, C., Parianos, J., Jones, D.O.B., 2019b. Preliminary observations of the abyssal megafauna of Kiribati. Front. Mar. Sci. 6, 605. https://doi.org/10.3389/fmars.2019.00605.

Swinbanks, D.D., 1982. *Paleodictyon*: the traces of an infaunal xenophyophore? Science 218 (4567), 47–49. https://doi.org/10.1126/science.218.4567.47.

Swinbanks, D.D., Shirayama, Y., 1986. High levels of natural radionuclides in a deep-sea infaunal xenophyophore. Nature 320, 354–357. https://doi.org/10.1038/320354a0.

Takahashi, K., 1998. The Bering and Okhotsk Seas: modern and past paleoceanographic changes and gateway impact. J. Asian Earth Sci. 16, 49–58. https://doi.org/10.1016/S0743-9547(97)00048-2.

Tendal, O.S., 1972. A monograph of the Xenophyophoria. Galathea Rep. 12, 7–103.

Tendal, O.S., 1996. Synoptic checklist and bibliography of the Xenophyophorea (Protista), with a zoogeographical survey of the group. Galathea Rep. 17, 79–101.

Tendal, O.S., Swinbanks, D.D., Shirayama, Y., 1982. A new infaunal xenophyophore (Xenophyophorea, Protozoa) with notes on its ecology and possible trace fossil analogues. Oceanol. Acta 5, 325–329.

Theising, F., Stoffers, T., Bong, F., Iwan, F., 2022. The SBE 32 Carousel Water Sampler (CTD). In: Brandt, A. (Ed.), SO293 AleutBio (Aleutian Trench Biodiversity Studies) Cruise Report/Fahrtbericht, Cruise No. SO293, 24.07.2022—06.09.2022, Dutch Harbor (USA) - Vancouver (Canada). In: SONNE-Berichte, SO293,. Begutachtungspanel Forschungsschiffe, Bonne, pp. 50–57.

Tsuchiya, M., Nomaki, H., 2021. Rapid response of the giant protist xenophyophores (Foraminifera, Rhizaria) to organic matter supply at abyssal depths revealed by an in situ dual stable isotope labelling experiment. Deep-Sea Res. I 176, 103608. https://doi.org/10.1016/j.dsr.2021.103608.

Tyler, P.A., 2003. The peripheral deep seas. In: Tyler, P.A. (Ed.), Ecosystems of the World 28. Ecosystems of the Deep Oceans. Elsevier, Amsterdam, Boston, London, New York, Oxford, Paris, San Diego, San Francisco, Singapore, Sydney, Tokyo, pp. 261–293.

Voltski, I., Weiner, A., Tsuchiya, M., Kitazato, H., 2018. *Syringammina limosa* sp. nov., the first xenophyophore from the deep Sea of Okhotsk: morphological and genetic description. Deep-Sea Res. II. https://doi.org/10.1016/j.dsr2.2017.12.001.